

NAUSIVIOS CHORA

A Journal in Naval Sciences and
Technology

PART C:

Natural Sciences and Mathematics



ΝΑΥΣΙΒΙΟΣ ΧΩΡΑ

Περιοδική Έκδοση Ναυτικών Επιστημών

ΜΕΡΟΣ Γ:

**Φυσικές Επιστήμες και
Μαθηματικά**

Volume 8/2022 - Τεύχος 8/2022

TABLE OF CONTENTS

C.J. Papachristou and A.N. Magoulas, Independence of Maxwell's equations: A Bäcklund-transformation view	C-3
Th. G. Douvropoulos, Field Induced Alteration of a Qubit's "Hadamard Time"	C-11
C.J. Papachristou, Approximate solutions of Maxwell's equations for a charging capacitor	C-47
A. Bacopoulos and D. Kouloumpou, MULTICRITERIA OPTIMIZATION Best Simultaneous Approximation of Functions	C-59

Independence of Maxwell's equations: A Bäcklund-transformation view

C. J. Papachristou ^(a) and A. N. Magoulas ^(b)

^(a) *Department of Physical Sciences, Hellenic Naval Academy*

^(b) *Department of Electrical Engineering, Hellenic Naval Academy*

Abstract. It is now widely accepted that the Maxwell equations of Electrodynamics constitute a self-consistent set of four independent partial differential equations. According to a certain school of thought, however, half of these equations – namely, those expressing the two Gauss' laws for the electric and the magnetic field – are redundant since they can be “derived” from the remaining two laws and the principle of conservation of charge. The status of the latter principle is thus elevated to a law of Nature more fundamental than, say, Coulomb's law. In this note we examine this line of reasoning and we propose an approach according to which the Maxwell equations may be viewed as a Bäcklund transformation relating fields and sources. The conservation of charge and the electromagnetic wave equations then simply express the integrability conditions of this transformation.

Keywords: Classical electrodynamics, Maxwell's equations, Bäcklund transformations

1. Is Gauss' law of Electrodynamics redundant?

As we know, the *Maxwell equations* describe the behavior (that is, the laws of change in space and time) of the electromagnetic (e/m) field. This field is represented by the pair (\vec{E}, \vec{B}) , where \vec{E} and \vec{B} are the electric and the magnetic field, respectively. The Maxwell equations additionally impose certain boundary conditions at the interface of two different media, while certain other physical demands are obvious (for example, the e/m field must vanish away from its localized “sources”, unless these sources emit e/m radiation).

The Maxwell equations are a system of four partial differential equations (PDEs) that is self-consistent, in the sense that these equations are compatible with one another. The self-consistency of the system also implies the satisfaction of two important conditions that are physically meaningful:

- the *equation of continuity*, related to *conservation of charge*; and
- the *e/m wave equation* in its various forms.

We stress that these conditions are *necessary but not sufficient* for the validity of the Maxwell system. Thus, although every solution (\vec{E}, \vec{B}) of this system obeys a wave

equation separately for the electric and the magnetic field, an arbitrary pair of fields (\vec{E}, \vec{B}) , each field satisfying the corresponding wave equation, does not necessarily satisfy the Maxwell system itself. Also, the principle of conservation of charge *cannot replace* any one of Maxwell's equations. These remarks are justified by the fact that the aforementioned two necessary conditions are derived by *differentiating* the Maxwell system and, in this process, part of the information carried by this system is lost. [Recall, similarly, that cross-differentiation of the Cauchy-Riemann relations of complex analysis yields the Laplace equation (see Sec. 2) by which, however, we cannot recover the Cauchy-Riemann relations.]

The differential form of the Maxwell equations is

$$\begin{aligned}
 (a) \quad \vec{\nabla} \cdot \vec{E} &= \frac{\rho}{\varepsilon_0} & (c) \quad \vec{\nabla} \times \vec{E} &= -\frac{\partial \vec{B}}{\partial t} \\
 (b) \quad \vec{\nabla} \cdot \vec{B} &= 0 & (d) \quad \vec{\nabla} \times \vec{B} &= \mu_0 \vec{J} + \varepsilon_0 \mu_0 \frac{\partial \vec{E}}{\partial t}
 \end{aligned} \tag{1}$$

where ρ, \vec{J} are the charge and current densities, respectively (the “sources” of the e/m field). Both the fields and the sources are functions of the spacetime variables (x, y, z, t) . Equations (1a) and (1b), which describe the *div* of the e/m field at any moment, constitute *Gauss' law* for the electric and the magnetic field, respectively. In terms of physical content, (1a) expresses the Coulomb law of electricity, while (1b) rules out the possibility of existence of magnetic poles analogous to electric charges. Equation (1c) expresses the *Faraday-Henry law* (law of e/m induction) and Eq. (1d) expresses the *Ampère-Maxwell law*. Equations (1a) and (1d), which contain the sources of the e/m field, constitute the *non-homogeneous* Maxwell equations, while Eqs. (1b) and (1c) are the *homogeneous* equations of the system.

By taking the *div* of (1d) and by using (1a), we obtain the *equation of continuity*, which physically expresses the *principle of conservation of charge* (see, e.g., [1], Sec. 9.6):

$$\vec{\nabla} \cdot \vec{J} + \frac{\partial \rho}{\partial t} = 0 \tag{2}$$

Although the charge and current densities on the right-hand sides of (1a) and (1d) are chosen freely and are considered known from the outset, relation (2) places a severe restriction on the associated functions. A different kind of differentiation of the Maxwell system (1), by taking the *rot* of (c) and (d), leads to separate wave equations (or modified wave equations, depending on the medium) for the electric and the magnetic field (see, e.g., [1], Sec. 10.4).

In most textbooks on electromagnetism (e.g., [2–6] and many more) the Maxwell equations (1) are treated as a consistent set of four independent PDEs. A number of authors, however, have doubted the independence of this system. Specifically, they argue that (1a) and (1b) – the equations for the *div* of the e/m field, expressing Gauss' law for the corresponding fields – are redundant since they “may be derived” from (1c) and (1d) in combination with the equation of continuity (2). If this is true, Coulomb's law – the most important experimental law of electricity – loses its status as an independent law and is reduced to a derivative theorem. The same can be said with regard to the non-existence of magnetic poles in Nature.

As far as we know, the first who doubted the independent status of the two Gauss' laws in electrodynamics was Julius Adams Stratton in his 1941 famous (and, admittedly, very attractive) book [7]. His reasoning may be described as follows:

By taking the *div* of (1c), the left-hand side vanishes identically while on the right-hand side we may change the order of differentiation with respect to space and time variables. The result is:

$$\frac{\partial}{\partial t}(\vec{\nabla} \cdot \vec{B}) = 0 \quad (3)$$

On the other hand, by taking the *div* of (1d) and by using the equation of continuity (2), we find that

$$\frac{\partial}{\partial t} \left(\vec{\nabla} \cdot \vec{E} - \frac{\rho}{\varepsilon_0} \right) = 0 \quad (4)$$

And the line of argument continues as follows: According to (3) and (4), the quantities $\vec{\nabla} \cdot \vec{B}$ and $(\vec{\nabla} \cdot \vec{E} - \rho / \varepsilon_0)$ are constant in time at every point (x, y, z) of the region Ω of space that concerns us. If we now assume that there has been a period of time during which no e/m field existed in the region Ω , then, in that period,

$$\vec{\nabla} \cdot \vec{B} = 0 \quad \text{and} \quad \vec{\nabla} \cdot \vec{E} - \rho / \varepsilon_0 = 0 \quad (5)$$

identically. Later on, although an e/m field did appear in Ω , the left-hand sides in (5) continued to vanish everywhere within this region since, as we said above, those quantities are time constant at every point of Ω . Thus, by the equations for the *rot* of the e/m field and by the principle of conservation of charge – the status of which was elevated from derivative theorem to fundamental law of the theory – we derived Eqs. (5), which are precisely the first two Maxwell equations (1a) and (1b)!

According to this reasoning, the electromagnetic theory is not based on four independent Maxwell equations but rather on *three* independent equations only; namely, the Faraday-Henry law (1c), the Ampère–Maxwell law (1d), and the principle of conservation of charge (2).

What makes this view questionable is the assumption that, for *every* region Ω of space there exists some period of time during which the e/m field in Ω vanishes. This hypothesis is arbitrary and is not dictated by the theory itself. (It is likely that no such region exists in the Universe!) Therefore, the argument that led from relations (3) and (4) to relations (5) is not convincing since it was based on an arbitrary and, in a sense, artificial initial condition: that the e/m field is zero at some time $t=0$ and before.

Let us assume for the sake of argument, however, that there exists a region Ω within which the e/m field is zero for $t < t_0$ and nonzero for $t > t_0$. The critical issue is what happens at $t=t_0$; specifically, whether the functions expressing the e/m field are *continuous* at that moment. If they indeed are, the field starts from zero and gradually increases to nonzero values; thus, the line of reasoning that led from (3) and (4) to (5) is acceptable. There are physical situations, however, in which the appearance of an e/m field is so abrupt that it may be considered *instantaneous*. (For instance, the moment we connect the ends of a metal wire to a battery, an electric field suddenly appears in the interior of the wire and a magnetic field appears in the exterior. An

even more “dramatic” example is *pair production* in which a charged particle and the corresponding antiparticle are created simultaneously, thus an e/m field appears at that moment in the region.) In such cases the e/m field is *non-continuous* at $t=t_0$ and its time derivative is *not defined* at this instant. Therefore, the line of reasoning that leads from (3) and (4) to (5) again collapses.

Note, finally, a circular reasoning in Stratton’s approach. It is assumed that, in a region Ω where no e/m field exists, the second of relations (5) is valid identically. This means that the vanishing of the electric field in Ω automatically implies the absence of electric charge in that region. This fact, however, follows from Gauss’ law (1a); thus it may not be used *a priori* as a tool for proving the law itself!

Regarding charge conservation, we mentioned earlier that Eq. (2) is derived from the two non-homogeneous Maxwell equations, namely, Gauss’ law (1a) for the electric field, and the Ampère–Maxwell law (1d). This means that the principle of conservation of charge is a *necessary* condition in order for the Maxwell system to be self-consistent. This condition is *not sufficient*, however, in the sense that it cannot replace any one of the system equations. Indeed, by the Ampère–Maxwell law and the conservation of charge there follows the *time derivative* of Gauss’ law for the electric field [Eq. (4)]; this, however, does not imply that Gauss’ law itself is valid. Of course, the reverse is true: *because* Gauss’ law is valid, the same is true for its time derivative.

Our view, therefore, is that the Maxwell equations form a system of four independent PDEs that express respective laws of Nature. Moreover, the self-consistency of this system imposes two *necessary* (but *not sufficient*) conditions that concern the conservation of charge and the wave behavior of the time-dependent e/m field. In the next section the problem is re-examined from the point of view of Bäcklund transformations.

2. A Bäcklund-transformation view of Maxwell’s equations

In previous articles [8,9] we suggested that, mathematically speaking, the Maxwell equations in empty space may be viewed as a Bäcklund transformation (BT) relating the electric and the magnetic field to each other. Let us briefly summarize a few key points regarding this idea. To begin with, let us see the simplest, perhaps, example of a BT.

The *Cauchy-Riemann relations* of complex analysis,

$$u_x = v_y \quad (a) \quad u_y = -v_x \quad (b) \quad (6)$$

(where subscripts denote partial derivatives with respect to the indicated variables) constitute a BT for the *Laplace equation*,

$$w_{xx} + w_{yy} = 0 \quad (7)$$

Let us explain this: Suppose we want to solve the system (6) for u , for a given choice of the function $v(x,y)$. To see if the PDEs (6a) and (6b) match for solution for u , we must compare them in some way. We thus differentiate (6a) with respect to y and (6b) with respect to x , and equate the mixed derivatives of u . That is, we apply the *integrability condition* (or *consistency condition*) $(u_x)_y = (u_y)_x$. In this way we eliminate the variable u and we find a condition that must be obeyed by $v(x,y)$:

$$v_{xx} + v_{yy} = 0.$$

Similarly, by using the integrability condition $(v_x)_y = (v_y)_x$ to eliminate v from the system (6), we find the necessary condition in order that this system be integrable for v , for a given function $u(x,y)$:

$$u_{xx} + u_{yy} = 0.$$

In conclusion, the integrability of system (6) with respect to either variable requires that the other variable satisfy the Laplace equation (7).

Let now $v_0(x,y)$ be a known solution of the Laplace equation (7). Substituting $v=v_0$ in the system (6), we can integrate this system with respect to u . It is not hard to show (by eliminating v_0 from the system) that the solution u will also satisfy the Laplace equation. As an example, by choosing the solution $v_0(x,y)=xy$ of (7), we find a new solution $u(x,y)=(x^2-y^2)/2+C$.

Generally speaking, a BT is a system of PDEs connecting two functions (say, u and v) in such a way that the consistency of the system requires that u and v independently satisfy the respective, higher-order PDEs $F[u]=0$ and $G[v]=0$. Analytically, in order that the system be integrable for u , the function v must be a solution of $G[v]=0$; conversely, in order that the system be integrable for v , the function u must be a solution of $F[u]=0$. If F and G happen to be functionally identical, as in the example given above, the BT is said to be an *auto-Bäcklund* transformation (auto-BT).

Classically, BTs are useful tools for finding solutions of nonlinear PDEs. In [8,9], however, we suggested that BTs may also be useful for solving *linear systems* of PDEs. The prototype example that we used was the Maxwell equations in empty space:

$$\begin{aligned} (a) \quad \vec{\nabla} \cdot \vec{E} &= 0 & (c) \quad \vec{\nabla} \times \vec{E} &= -\frac{\partial \vec{B}}{\partial t} \\ (b) \quad \vec{\nabla} \cdot \vec{B} &= 0 & (d) \quad \vec{\nabla} \times \vec{B} &= \varepsilon_0 \mu_0 \frac{\partial \vec{E}}{\partial t} \end{aligned} \tag{8}$$

Here we have a system of four PDEs for two vector fields that are functions of the spacetime coordinates (x,y,z,t) . We would like to find the integrability conditions necessary for self-consistency of the system (8). To this end, we try to uncouple the system to find separate second-order PDEs for \vec{E} and \vec{B} , the PDE for each field being a necessary condition in order that the system (8) be integrable for the other field. This uncoupling, which eliminates either field (electric or magnetic) in favor of the other, is achieved by properly differentiating the system equations and by using suitable vector identities, in a manner similar in spirit to that which took us from the first-order Cauchy-Riemann system (6) to the separate second-order Laplace equations (7) for u and v .

As discussed in [8,9], the only nontrivial integrability conditions for the system (8) are those obtained by using the vector identities

$$\vec{\nabla} \times (\vec{\nabla} \times \vec{E}) = \vec{\nabla} (\vec{\nabla} \cdot \vec{E}) - \nabla^2 \vec{E} \tag{9}$$

$$\vec{\nabla} \times (\vec{\nabla} \times \vec{B}) = \vec{\nabla} (\vec{\nabla} \cdot \vec{B}) - \nabla^2 \vec{B} \quad (10)$$

By these we obtain separate wave equations for the electric and the magnetic field:

$$\nabla^2 \vec{E} - \varepsilon_0 \mu_0 \frac{\partial^2 \vec{E}}{\partial t^2} = 0 \quad (11)$$

$$\nabla^2 \vec{B} - \varepsilon_0 \mu_0 \frac{\partial^2 \vec{B}}{\partial t^2} = 0 \quad (12)$$

We conclude that the Maxwell system (8) in empty space is a BT relating the e/m wave equations for the electric and the magnetic field, in the sense that the wave equation for each field is an integrability condition for solution of the system in terms of the other field.

The case of the full Maxwell equations (1) is more complex due to the presence of the source terms ρ, \vec{J} in the non-homogeneous equations (1a) and (1d). As it turns out, the self-consistency of the BT imposes restrictions on the terms of non-homogeneity as well as on the fields themselves. Before we get to this, however, let us see a simpler “toy” example that generalizes that of the Cauchy-Riemann relations.

Consider the following non-homogeneous linear system of PDEs for the functions u and v of the variables x, y, z, t :

$$\begin{aligned} u_x = v_y & \quad (a) & u_z = v_z + p(x, y, z, t) & \quad (c) \\ u_y = -v_x & \quad (b) & u_t = v_t + q(x, y, z, t) & \quad (d) \end{aligned} \quad (13)$$

where p and q are assumed to be given functions. The necessary consistency conditions for this system are found by cross-differentiation of the system equations with respect to the variables x, y, z, t . In particular, by cross-differentiating (a) and (b) with respect to x and y we find that $u_{xx} + u_{yy} = 0$ and $v_{xx} + v_{yy} = 0$; hence both u and v must satisfy the Laplace equation (7). On the other hand, cross-differentiation of (c) and (d) with respect to z and t eliminates the fundamental variables u and v , yielding a necessary condition for the terms of non-homogeneity, p and q ; that is, $p_t - q_z = 0$. This means that the functions p and q cannot be chosen arbitrarily from the outset but must conform to this latter condition in order for the system (13) to have a solution.

As an application, let us take $v = xy + zt$ (which satisfies the Laplace equation $v_{xx} + v_{yy} = 0$) and let us choose $p = 2t$ and $q = 2z$ (so that $p_t - q_z = 0$). It is not hard to show that the solution of the system (13) for u is then given by

$$u(x, y, z, t) = (x^2 - y^2)/2 + 3zt + C.$$

Notice that $u_{xx} + u_{yy} = 0$, as expected.

Let us now return to the full Maxwell equations (1), which we now view as a BT relating the electric and the magnetic field and containing additional terms in which only the sources appear. As can be checked, there are now three nontrivial integrability conditions, namely, those found by applying the vector identities (9) and (10), as well as the identity

$$\vec{\nabla} \cdot (\vec{\nabla} \times \vec{B}) = 0 \quad (14)$$

(the corresponding one for \vec{E} is trivially satisfied in view of the Maxwell system). By (9) and (10) we get the non-homogeneous wave equations

$$\nabla^2 \vec{E} - \varepsilon_0 \mu_0 \frac{\partial^2 \vec{E}}{\partial t^2} = \frac{1}{\varepsilon_0} \vec{\nabla} \rho + \mu_0 \frac{\partial \vec{J}}{\partial t} \quad (15)$$

$$\nabla^2 \vec{B} - \varepsilon_0 \mu_0 \frac{\partial^2 \vec{B}}{\partial t^2} = -\mu_0 \vec{\nabla} \times \vec{J} \quad (16)$$

Additionally, the integrability condition (14) yields the equation of continuity (2),

$$\vec{\nabla} \cdot \vec{J} + \frac{\partial \rho}{\partial t} = 0 \quad (17)$$

expressing conservation of charge. Notice that, unlike (15) and (16), the condition (17) places *a priori* restrictions on the sources rather than on the fields themselves!

In any case, the three relations (15) – (17) are *necessary* conditions imposed by the requirement of self-consistency of the BT (1). As explained in Sec. 1, however, these conditions are *not sufficient*, in the sense that none of them may replace any equation in the system (1). In particular, the equation of continuity (17) may not be regarded as more fundamental than the Gauss law (1a) for the electric field.

3. Conclusions

Let us summarize our main conclusions:

1. The Maxwell equations (1) express four separate laws of Nature. These equations are mathematically consistent with one another but constitute a set of independent vector relations, in the sense that no single equation may be deduced by the remaining three. In particular, the physical arguments that attempt to render the two Gauss' laws “redundant” are seen to be artificial and unrealistic.

2. We consider the Maxwell equations as physically acceptable simply because the system (1) and all conclusions mathematically drawn from it represent experimentally verifiable situations in Nature. Among these conclusions are the conservation of charge and the conservation of energy (Poynting's theorem). It should be kept in mind, however, that conservation laws appear as *consequences* of the fundamental equations of a theory, and not vice versa. In particular, conservation of charge, in the form of the continuity equation (17), is a physically verifiable mathematical conclusion drawn from the Maxwell system (1) but it may not be regarded as more fundamental than any equation in the system. The same can be said with regard to the existence of e/m waves, expressed mathematically by Eqs. (11) and (12).

3. From a mathematical perspective, the Maxwell system (1) may be viewed as a Bäcklund transformation (BT) the integrability conditions of which (i.e., the *necessary* conditions for self-consistency of the system) yield separate (generally non-

homogeneous) wave equations (15) and (16) for the electric and the magnetic field, respectively, as well as the equation of continuity (17). These integrability conditions are derived by *differentiating* the BT in different ways; hence they carry less information than the BT itself. Consequently, none of the integrability conditions may replace any equation in the Maxwell system.

Acknowledgment

We thank Dr. Norman H. Redington of MIT for suggesting future directions for this research.

References

1. C. J. Papachristou, *Introduction to Electromagnetic Theory and the Physics of Conducting Solids* (Springer, 2020).¹
2. J. D. Jackson, *Classical Electrodynamics*, 3rd Edition (Wiley, 1999).
3. W. K. H. Panofsky, M. Phillips, *Classical Electricity and Magnetism*, 2nd Edition (Addison-Wesley, 1962).
4. D. J. Griffiths, *Introduction to Electrodynamics*, 4th Edition (Pearson, 2013).
5. R. K. Wangsness, *Electromagnetic Fields*, 2nd Edition (Wiley, 1986).
6. W. N. Cottingham, D. A. Greenwood, *Electricity and Magnetism* (Cambridge, 1991).
7. J. A. Stratton, *Electromagnetic Theory* (McGraw-Hill, 1941).
8. C. J. Papachristou, *The Maxwell equations as a Bäcklund transformation*, *Advanced Electromagnetics*, Vol. 4, No. 1 (2015), pp. 52-58.²
9. C. J. Papachristou, A. N. Magoulas, *Bäcklund transformations: Some old and new perspectives*, *Nausivios Chora*, Vol. 6 (2016) pp. C3-C17.³

¹ <https://arxiv.org/abs/1711.09969>

² <http://www.aemjournal.org/index.php/AEM/article/view/311>

³ <http://nausivios.snd.edu.gr/docs/2016C.pdf>

Field Induced Alteration of a Qubit's “Hadamard Time”

Theodosios Geo Douvropoulos

*Hellenic Naval Academy, Physical Sciences Sector, Pure & Applied Physics,
Hatzikyriakou Ave. Piraeus, 18539, Greece
douvrotheo@yahoo.com*

Abstract. In this paper, we explore the dynamics of a qubit state prepared in a double-well potential generated by the coupling of the system with the environment through two independent field barriers. Thus, we adopt the path-integral theory to reveal the system's complex energy spectrum through the construction of its Green's function. In particular, we focus on the alteration of the “Hadamard Time” defined in the current paper. We qualitatively study the aforementioned alteration as a function of various parameters, such as the magnitude of the field barriers, the relative size of the well related to the internal barrier, and the shape similarity factor. We analytically define these quantities inside the manuscript. We also discuss in detail the appearance of the exponential decay rate. Since our results come in analytic form, they permit their future numerical application in realistic physical and quantum computing systems.

Keywords: Qubit, Hadamard Gate, Superposition State, Beam Splitter, Double Well Potential (DWP), Path Integral Method, Inversion Period, Exponential Decay Rate, Decoherence

PACS: 03.65.-w, 03.65.Sq, 03.65.Xp

INTRODUCTION

The qubit, which is the quantum version of the classical bit [1], corresponds to a class of quantum systems possessing a characteristic property that can admit two possible values. In general we focus our attention on this property and consider the rest as frozen or out of interest. Thus considering the spin of an electron, the two possible values are namely the spin up and spin down while considering the

polarization of a photon, the horizontal and vertical polarization, [2,3]. As far as the position of an atom or electron is concerned, the double well potential serves as a one dimensional qubit where the atom or electron can be found in the left or right well. Spin qubits can be realized by either solid-state or superconductor technology [4,5], and at the same time position qubits (for instance the presence or absence of an electron in a quantum dot) which are known as charge or electrostatic qubits, can also be implemented either in a semiconductor manner [6,7] or using a Cooper pair box [8,9] in superconductors. A combination of the above deals with the use of hybrid spin-charge superconducting qubits, e.g. transmons, [10]. The interested reader may find a review of the current semiconductor and super-conducting technologies in [11,12].

The one-dimensional double well potential (DWP), depicted by Figure 3 that follows, not only stands throughout the ages as a model for the study of some peculiar but still most basic quantum phenomena, such as internal tunneling and energy splitting, but at the same time is a widely used practical model for the study of a variety of systems and processes in Physical Sciences. Out of the plethora of such studies, we distinguish the Ammonia maser [13,14], the Bose Einstein condensates [15-17], structural phase transitions [18], matter-wave interferometry in atomic dimensions [19], realization of qubits, [20], and realization of beam splitters [21].

Quantum computation strongly relies on the realization, manipulation and control of qubits. As far as the realization is concerned, a basic technique deals with the construction of a double - well potential in such a way that the energies of its first two eigenstates appear to have a large gap with the rest, [22,23]. For example holes in quantum wells have the attractive property of a light effective mass which is highly desirable for spin qubits since it provides large energy level spacing in quantum dots, [24]. In addition it is well known from the late 90s that we can use linear components of quantum optics technology, such as lossless symmetric beam splitters, for the implementation of universal quantum gates such as the Hadamard gate, and to further perform precisely the computation of quantum gates and algorithms, [25]. A Bose Einstein Condensate beam splitter uses condensates instead of single particles and can be realized with a DWP of tunable height, [21].

A single particle qubit implemented as a DWP, can be built up from two coupled semiconductor quantum dots, where the band offset of different materials in one direction results in an effective one dimensional DWP, [26-28]. Alternatively it can be built up through the use of superconductor devices based on the Josephson effect, where the effective DWP results via a RF-SQUID circuit [29-31]. A third option comes from trapped ions in a DWP which are confined via the use of strong magnetic and electric fields, [33-35]. However it is extremely difficult to confine a trapped ion in different topology than the one of a in-line arrangement providing a low scalability and in addition just as other quantum processors they demand extremely low temperatures. Despite the complexity of the above mentioned systems, their basic structure and dynamics can be explained through basic principles of the one dimensional DWP, [35-37].

Thus, during the recent years many different schemes both theoretical and experimental have been proposed for the implementation and manipulation of qubits through effective one dimensional DWP. Mentioning a few we distinguish the analysis of the phase evolution of the Cooper pairs wave function for obtaining a DWP with cusp barriers for current qubits, [38], the DWP Josephson junction between two d-wave superconductors, as an implementation of a phase or flux qubit, [39], the analysis for designing a vortex qubit created in a DWP in a semiannular

Josephson junction, [40,41], buckling nanobars which are nano-electromechanical quantum coherent systems as to be forming a DWP for charge qubits, [42], quantum dots in semiconductor nanocolumns prepared by epitaxial growth and where the carrier confinement in the direction of the DWP can be achieved by conformal overgrowth of a semiconductor barrier layer, [43], and many others.

A suitably engineered quantum well can stabilize the charge state of the qubit against photoionization [44] and when an electric field is imposed on the DWP the induced lack of inversion symmetry allows the possibility of different qubit manipulation methods such as electron spin resonance, electric dipole spin resonance and g-tensor modulation resonance, [45]. On the other hand the most exotic phenomena of quantum mechanics such as quantum entanglement can be produced through a DWP qubit and its interaction with a source of non classical light, [46]. In addition, single and two-qubit operations can be realised through a high degree of control over the tunnel coupling of the DWP, while spin-orbit coupling obviates the need for microscopic elements and enables rapid qubit control through fast rotations, [47].

As far as the dynamics of the qubit is concerned, decoherence was understood to play a key role at the very beginning of quantum computation, [48]. Coherence time refers to the length of time that a quantum superposition state can survive. The key is to have a quantum superposition live longer than it takes to perform an operation or experiment. Manipulation of the qubit destroys isolation and induces decoherence of its state. It is experimentally observed that spin-based qubits maintain coherence for a longer time length than electrostatic qubits [49].

Hence, all the above motivated us for producing the current work. In this paper we study the dynamics, meaning the time evolution, of a qubit state in a DWP, which is a potential that possesses two minima separated by an internal barrier, under the additional influence of a two channel (barrier) field, as this is depicted by Figure 2 that follows. In a way, it continues previous works of ours on the DWP, [50,51]. Such a model adds to the normal dynamics of the DWP the possibility of irreversible dissipation to the free particle continuum. The work described in this paper, constitutes a particular implementation of the path integral method to the model potential which is depicted by Figure 2, where a barrier field is inserted in each side of the unperturbed potential of the qubit, in order to qualitatively describe not only the field-induced variation of energy splitting and/or time period of internal oscillation, but the appearance of exponential decay rates as well, describing the dissociation of the qubit. However we should have in mind, that when it comes to application, most of the formal and mathematical work uses arbitrary parameters. Therefore, the interesting information of such calculations is not in the absolute value of the numbers, since it is hard to see how experimental conditions and measurements can test exactly the model problem. In addition, the present treatment has allowed the derivation of analytic formulas for the energies, the energy shifts, and energy widths, due to tunneling. Such a potential has not been treated before analytically, making the problem rather challenging.

The present paper is organized as follows. In the first section we describe in short the path integral method to be applied, for the construction of the qubit's Green's function, introducing the various phase factors to be used. Next we actually apply the method and gradually construct the qubit's Green's function, by taking in account the various phase factors that the system's topology acquires through successive propagation and reflection events. We also carry out the tedious algebra and calculate the qubit's Green's function in a compact fractional form. In the third section we

briefly review the dynamics (time evolution) of the DWP and define the Hadamard Time. Next we bring out the significance of its energy spectrum, as far as the energy splitting and the Hadamard Time are concerned. In the fourth section we reveal the system's complex energy spectrum, while in the next section we analyze the dynamics of the model studied, concerning the alteration of the Hadamard Time and the exponential decay rate, for various values of the parameters used. In this section we introduce quantity $sim(\widehat{\xi}, \bar{\mathcal{G}})$ that measures the shape of the qubit's internal barrier relative to the one of its well. In the final section we conclude, and light our most important results.

THE CONSTRUCTION OF THE QUBIT'S GREEN'S FUNCTION VIA PATH INTEGRALS

As is well known, both the Schrodinger and Heisenberg picture in Quantum Mechanics, deal with the basic dynamical differential equations involving either the states or the operators, [52]. In deep contrast, Feynman's formulation of path integration [53], offers an alternative geometric picture and targets directly towards the solution of the Schrodinger equation, which is constructed in the form of a propagator.

Feynman showed how a system's propagator can be determined by the "sum over histories", meaning quantity

$$K_F = N \int e^{iS(x(t))/\hbar} Dx(t) \quad (1)$$

where the above functional expresses the sum over the classical paths and S stands for the classical action. Thus, the square meter of the propagator, which is $|K(x, t_2 ; x_1, t_1)|^2$, gives the probability of finding the particle at the time t_2 , assuming the starting and ending point to be x_1 and x_2 respectively. Its energy Fourier transform, called the fixed energy amplitude [54], is the system's Green's function $K(E)$. Its construction reveals the energy spectrum of the system under study, since the Green's function can be written as a sum of energy pole terms of the following form

$$K(E) \sim \sum_n \frac{c_n}{E - Z_n} \quad (2)$$

The Z_n energy poles may be real or complex, depending on the dynamics of the system under study.

In their periodic orbit theory, Gutzwiller [56] and later Miller [57,58], showed the way Green's function can be constructed for one dimensional propagation, via the calculation of all the possible changes in phase of the wave-function through the corresponding changes of the action, during the system's propagation over the classical paths. Holstein [59] in his seminal work, put all these together, and nicely showed how the fixed energy amplitude, can be used to achieve analytic continuation

of the propagator to forbidden regions of motion, (potential barriers), where the particle travels in imaginary times. His central result for the calculation of the transmission amplitude via an infinite set of paths that the particle follows, can be written in the compact form that follows

$$K(E) = \sum_{j=1}^{\infty} \left\{ \prod_{i=1}^{N(j)} \frac{m}{\hbar^2 k_{r_1} k_{r_2}} s_{ij}^{2\pi} \right\} \quad (3)$$

In the above equation $k_{r_1} k_{r_2}$ is a non local wave number of the particle connecting the initial and the final point of propagation and defined by

$$k_{r_1} k_{r_2} \equiv \sqrt{k(r_1)k(r_2)} \quad (4)$$

where $k(y) = \sqrt{2m(E - V(y))/\hbar^2}$, with E standing for the energy and $V(y)$ for the potential function. The index j corresponds to a particular path, while the index i corresponds to a certain event along the path. Therefore, the symbol $s_{ij}^{2\pi}$ represents each i event factor that contributes to the j^{th} path normalized to the maximum change in phase which is equal to 2π . Their total number is $N(j)$ and depends on the path. These event factors are of two types. One type represents propagation and the other represents reflection from a turning point.

The $s_{ij}^{2\pi}$ propagation event phase factors describe propagation (from a to b) in an either allowed region (given by $\exp\left[i \int_a^b k(y) dy\right] \equiv e^{i\tilde{g}(b)} \equiv \tilde{g}_b$, where the \cup superscript stands for the shape of the well), or in a forbidden region (from b to c) of motion (given by $\exp\left[-i \int_b^c \lambda(y) dy\right] \equiv e^{-\tilde{\xi}(b)} \equiv \tilde{\xi}_b$ with $\lambda(y) = \sqrt{2m(V(y) - E)/\hbar^2} = ik(y)$, where the \cap superscript stands for the shape of the barrier). The dimensionless phase quantities $\tilde{g}(b)$ and $\tilde{\xi}(b)$ will be called the ‘‘qubit well magnitude’’ (qwm) and the ‘‘qubit barrier magnitude’’ (qbm) respectively. A large qwm corresponds to a deep and broad potential well while a large qbm corresponds to a high and broad potential barrier. These quantities appear continuously in the text and figures that follow and play a significant role in the qubit’s dynamics since the first contributes to the oscillation of its orthogonal basis states and the second to the tunneling phenomenon. The $s_{ij}^{2\pi}$ reflection event phase factors describe reflections from turning points, ($-i$ for reflection from a turning point in an allowed region, $+i/2$ for reflection in a forbidden region, and -1 for reflection from an infinite barrier).

However, someone notes that the reflection factors (except of course for the case of an infinite barrier), do not take in account the relative size of the involved areas. For example if a particle is reflected back to a classically allowed region of motion, the reflection factor will always be equal to $(-i)$, no matter how large is in magnitude the potential barrier on the other side of the turning point. Clearly, this is an issue that has to be solved and it actually does in the context of the present research, as will be seen later. Both $\tilde{g}(b)$ and $\tilde{\xi}(b)$ are dimensionless phase quantities. The above mentioned rules are in total depicted by Figure 1 that follows and can also be found in standard textbooks of path integrals, or quantum tunneling as well, [54,60]. For the

present requirement of computing the overall transmission amplitude, the points r_1 and r_2 are in the classically allowed region of motion of the left well of Figure 2.

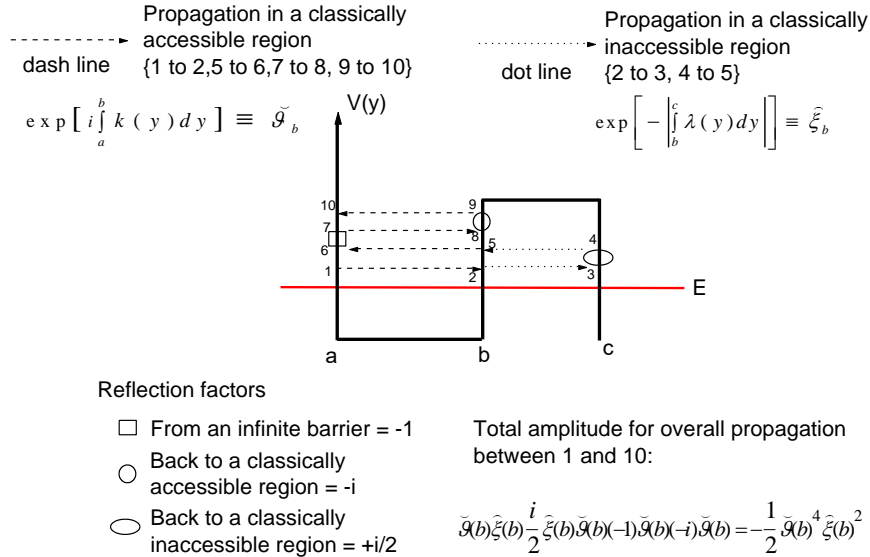


FIGURE 1. The rules for the construction of the path integral amplitudes through the $s_{ij}^{2\pi}$ event factors. Here we depict a path example involving 9 event phase factors. The dash line stands for propagation in a classically allowed region, while the dot line for propagation in a classically inaccessible region. These regions are characterised so by the relative value of the energy. The square reflection factor (-1) stands for reflection from an infinite barrier, the circle reflection factor (-i) for reflection back to a classically allowed region and the elliptic reflection factor (+i/2) for reflection back to a classically inaccessible region.

As far as the model is considered to have only one degree of freedom, corresponding to the relative position of the atom or electron, it can be treated as a one dimensional physical system. Thus we can apply the path integral method for the construction of the Green's function. In addition we should sketch the perturbed one dimensional potential as in Figure 2 that follows:

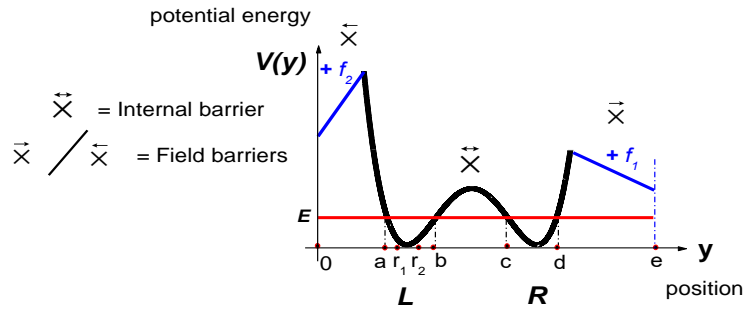


FIGURE 2. The potential of a perturbed double well. There are five regions of motion: the classically accessible regions L and R corresponding to states $|0\rangle$ and $|1\rangle$, and the classically inaccessible regions \bar{x} , \bar{x} , \bar{x} of the internal and the field barriers respectively. The blue lines f_1 and f_2 stand for the electrostatic field imposed on the right and left well respectively while E stands for the particle's energy. The slope of f_1 and f_2 is proportional to the corresponding field strength. There are four turning points of motion (a,b,c,d) and points r_1 and r_2 lie between a and b of the left well.

Figure 2 describes the induced topology of the potential as this is determined by the specific value of the energy. There are four turning points, meaning a, b, c, and d. In this way we have five regions of motion, two classically allowed (L and R wells) and three classically forbidden (barriers \bar{x} , \bar{x} , \bar{x}). In order to construct the overall transition amplitude for propagation between points r_1 and r_2 of region L, we divide the problem into simpler ones.

For this we write $K(E)$ as a sum of transition amplitudes involving specific regions of motion each time, of the form:

$$K(E) = \frac{m}{\hbar^2 k_{r_1; r_2}} \left\{ \Upsilon^L + \Upsilon^{L, \bar{x}} + \Upsilon^{L, \bar{x}, |1\rangle} + \Upsilon^{L, \bar{x}, R, \bar{x}} + \Upsilon^{L, \bar{x}, R, \bar{x}, \bar{x}} \right\} \quad (5)$$

where $\Upsilon^{L, \bar{x}, R}$ for example denotes the amplitude for propagation involving the classically allowed regions L and R as well as the internal barrier, in all possible ways. Table 1 that follows explains the symbols that we will use in the rest of the manuscript, concerning the various amplitudes.

SYMBOL	DESCRIPTION
\tilde{g}_r	Contribution of a single propagation in a classically allowed region as a function of the ending point r for starting point a
$\tilde{\xi}_b$	Contribution of a single propagation in a classically forbidden region as a function of the starting point b
$\vec{A}_q(r_1; r_2)$	Amplitude for a single propagation from left to right inside region q between points r_1 and r_2
$A_q(r_1; r_2)$	Amplitude for infinite repetitions of the propagation between r_1 and r_2 in all possible ways, while staying at region q
$\{p \rightleftarrows_{r_1}^{r_2} q\}$	Overall amplitude for exhausting combination of the regions p and q propagating between r_1 and r_2
$\Upsilon^{p,q}$	Total contribution to the Green's function through the exclusive combination of regions p and q

TABLE 1. Basic symbols and their definition, in the current manuscript.

In Appendix A we separately develop each amplitude of eq.(4) providing the basic steps. In the lines that follow we give an example by calculating the contribution of the L well. Transition Amplitude Υ^L involves propagation inside the classically allowed region of the left potential well where the state $|0\rangle$ lives. It is constructed by fundamental amplitudes, for example $\vec{A}_L(r;a)$ that connects points r and a in a single straight path moving from right to left, (the arrow denotes direction), and by amplitudes $A_L(r;a)$, that connect r and a with infinite repetitions (including reflections) in all possible ways. In this way we can write:

$$\begin{aligned} \Upsilon^L = & \vec{A}_L(r_1; r_2) + \vec{A}_L(r_1; a)(-i) \{ A_L(a; a)(-i) \vec{A}_L(a; r_2) + A_L(a; b)(-i) \vec{A}_L(b; r_2) \} \\ & + \vec{A}_L(r_1; b)(-i) \{ A_L(b; b)(-i) \vec{A}_L(b; r_2) + A_L(b; a)(-i) \vec{A}_L(a; r_2) \} \end{aligned} \quad (6)$$

Table 2 that follows contains the calculation of the above mentioned fundamental amplitudes:

Fundamental amplitudes of area L	Function of event phase factors
$\vec{A}_L(r_1; r_2)$	$\vec{g}_{r_2} / \vec{g}_{r_1}$
$\vec{A}_L(r_1; a)$	\vec{g}_{r_1}
$\vec{A}_L(r_1; b)$	$\vec{g}_b / \vec{g}_{r_1}$
$\vec{A}_L(a; r_2)$	\vec{g}_{r_2}
$\vec{A}_L(b; r_2)$	$\vec{g}_b / \vec{g}_{r_2}$
$A_L(a; a)$	$\{2 \operatorname{Re}(\vec{g}_b) \vec{g}_b\}^{-1}$
$A_L(a; b)$	$\{2 \operatorname{Re}(\vec{g}_b)\}^{-1}$

TABLE 2. Calculation of the amplitudes involved in the propagation inside region L.

Giving a second example, the $A_L(a; a)$ amplitude comes from the infinite repetition of the $(a; a)$ propagation, including the reflection factors, which is

$$A_L(a; a) = 1 + \vec{g}_b(-i) \vec{g}_b(-i) + \dots = \frac{1}{1 + \vec{g}_b^2} = \frac{1}{2 \operatorname{Re} \vec{g}_b} \quad (7)$$

It is also clear that

$$A_L(a; b) = \vec{g}_b A_L(a; a) = \frac{1}{2 \operatorname{Re} \vec{g}_b} \quad (8)$$

Putting all these together we get for the Υ^L amplitude the following expression

$$\Upsilon^L = \vec{g}_{r_2} / \vec{g}_{r_1} + \frac{1}{1 + \vec{g}_b^2} \left\{ -i \frac{\vec{g}_b^2}{\vec{g}_{r_2} \vec{g}_{r_1}} - \vec{g}_b^2 \frac{\vec{g}_{r_1}}{\vec{g}_b} - i \vec{g}_{r_2} \vec{g}_{r_1} \right\} \quad (9)$$

Introducing $\vec{g}_b^{\pi/4} = i^{1/2} \vec{g}_b$ we finally get for the Υ^L amplitude

$$\Upsilon^L = -2i \frac{\operatorname{Im} \vec{g}_{r_1}^{\pi/4}}{\vec{g}_{r_2}^{\pi/4}} + \frac{2 \operatorname{Im} \vec{g}_{r_1}^{\pi/4} \operatorname{Im} \vec{g}_{r_2}^{\pi/4}}{\vec{g}_b \operatorname{Re} \vec{g}_b} \quad (10)$$

Equation A.15 of Appendix A gives Green's function for the total amplitude contribution, as

$$K(E) = \frac{m}{\hbar^2 k_{r_1; r_2}} \left\{ \frac{1}{2 \left\{ 1 - \Upsilon^{L+\vec{x}+R+\vec{x}}(r_1; a) A_{\vec{x}}(a; a) \right\} \vec{g}_b \operatorname{Re} \vec{g}_b} \right\} \quad (11)$$

where the amplitude $\Upsilon^{L+\vec{x}+R+\vec{x}}$ is defined by equation A.12 of Appendix A and given as

$$\Upsilon^{L+\bar{x}+R+\bar{x}} = -2i \frac{\text{Im} \tilde{\mathcal{G}}_1^{\pi/4}}{\tilde{\mathcal{G}}_2^{\pi/4}} + \frac{2 \frac{\text{Im} \tilde{\mathcal{G}}_1^{\pi/4} \text{Im} \tilde{\mathcal{G}}_2^{\pi/4}}{\tilde{\mathcal{G}}_b}}{4 \text{Re} \tilde{\mathcal{G}}_b - \tilde{\xi}_b^2 \tilde{\mathcal{G}}_b \pm \frac{1}{\tilde{\mathcal{G}}_b} \left\{ -4 \tilde{\xi}_b^2 \tilde{\mathcal{G}}_b^4 + \frac{(4 \tilde{\xi}_b \tilde{\gamma}_d)^2 \tilde{\mathcal{G}}_b^3 \text{Re} \tilde{\mathcal{G}}_b}{(4 \text{Re} \tilde{\mathcal{G}}_b - \tilde{\xi}_b^2 \tilde{\mathcal{G}}_b)^2 + (\tilde{\xi}_b \tilde{\gamma}_d)^2} \right\}^{1/2}} \quad (12)$$

and the field barriers \bar{x} and \bar{x} acquire phase factors to form the following barrier

$$\text{magnitudes } \exp \left[- \left| \int_d^e \tau(y) dy \right| \right] \equiv e^{-\gamma(d)} \equiv \tilde{\gamma}_d \text{ and } \exp \left[- \left| \int_0^a \tau(y) dy \right| \right] \equiv e^{-\delta(a)} \equiv \tilde{\delta}_a$$

respectively, and where of course $A_x(a; a) = \frac{i}{2} \frac{\tilde{\delta}_a^2}{1 + \tilde{\delta}_a^2/4}$.

SHORT REVIEW OF THE TIME EVOLUTION OF A QUANTUM STATE IN A DOUBLE WELL POTENTIAL

In the present chapter we briefly review the dynamics concerning the time evolution of a quantum state in a double well structure, as this can be found in any standard textbook of quantum mechanics and quantum tunneling [14,61]. For this, we assume to have the two initially separated lowest, degenerate eigenstates of the two independent unperturbed wells, namely $|0\rangle$ and $|1\rangle$ with energy E_o , that do not overlap with each other, as depicted by Figure 3 that follows. These states will interact through the finite potential barrier that separates the two wells to construct the eigenfunctions of the DWP. Since the potential is an even function, its Hamiltonian commutes with the parity operator. Thus we can construct an orthonormal basis of symmetric and antisymmetric states, as follows

$$S = \frac{1}{\sqrt{2}} \{|0\rangle + |1\rangle\} \quad \text{and} \quad A = \frac{1}{\sqrt{2}} \{|0\rangle - |1\rangle\} \quad (13)$$

In fact we can mathematically describe the finite potential barrier as a perturbation matrix of the form $U = -\delta \sigma_x$, [62], where of course σ_x stands for the Pauli matrix:

$$\sigma_x = \begin{pmatrix} 0 & 1 \\ 1 & 0 \end{pmatrix} \quad (14)$$

Hence the total Hamiltonian becomes equal to $H = \begin{pmatrix} E_o & -\delta \\ \delta & E_o \end{pmatrix}$. Diagonalization of the Hamiltonian gives two new eigenvalues for the symmetric and antisymmetric state, which are respectively: $E_S = E_o - \delta$ and $E_A = E_o + \delta$, whose energy distance is equal to $\Delta = 2\delta$. Thus, the degeneration of the two initial states is removed, and an energy splitting appears of the corresponding energy levels.

Let us assume now that at $t=0$ the system is prepared in the state $|0\rangle$ of the left well, which can be written as a superposition of states of the DWP:

$\Psi(t=0) = |0\rangle = \frac{1}{\sqrt{2}}\{S + A\}$. The time evolution of the state will then be $\Psi(t) = \frac{1}{\sqrt{2}}\{e^{-it(E_o-\delta)/\hbar}S + e^{-it(E_o+\delta)/\hbar}A\}$. In terms of the initial eigenfunctions of the two separate wells, we can write

$$\Psi(t) = e^{-itE_o/\hbar} \{ \cos(\delta t / \hbar) |0\rangle + i \sin(\delta t / \hbar) |1\rangle \} \quad (15)$$

We particularly focus on the ‘‘Hadamard Time’’, defined as the time needed for the initial state of the qubit ($|0\rangle$ or $|1\rangle$) to come in an equally weighted superposition of the two complementary orthogonal states, $|0\rangle$ and $|1\rangle$. In the context of the present research activity this time is defined as the Hadamard Time, since the action of the Hadamard gate on $|0\rangle$ is actually $H|0\rangle = \frac{1}{\sqrt{2}}\{|0\rangle + |1\rangle\}$. Thus, the time needed for the initial state $|0\rangle$ to come in an equally weighted superposition of itself and its complementary state $|1\rangle$ is equal to

$$T_{Hd} = \frac{h}{4\Delta} \quad (16)$$

Hadamard Time comes as a function of the energy difference of the two lower states of the DWP. Thus, in order to explore the system’s dynamics under the action of the two field barriers, we must first analyze its energy spectrum. The diffusion of the initial state to the continuum set of states through the field barriers, turns the spectrum into complex. Hence, the real part of the spectrum determines the alteration of the Hadamard Time while the imaginary part determines the state’s decay rate to the continuum, meaning decoherence.

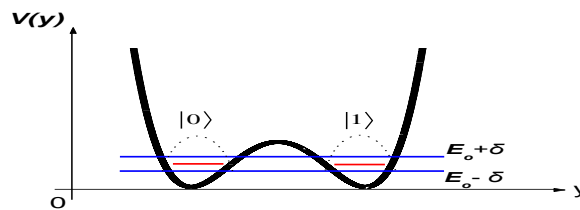


FIGURE 3. The doublet splitting in a DWP. The two initially degenerate states $|0\rangle$ and $|1\rangle$ with energy E_o of the two separate unperturbed wells, interact through the internal potential barrier \vec{x} and form the symmetric (S) and antisymmetric states (A) of the full potential, with energies $E_o - \delta$ and $E_o + \delta$ respectively.

THE ENERGY SPECTRUM OF THE FIELD PERTURBED DOUBLE WELL

As we have already seen, the step by step construction of the total Green's function, reveals gradually additional fractional pole terms, coming as the extra contribution of each new region of motion. In turn, these poles correspond to the energies of the system due to the qubit interaction with the field barriers.

Thus, for each fractional contribution of the total Green's function, we need to expand the denominator around the eigenvalues E_n of the unperturbed well. In this way, we calculate the energy shift that takes place, coming from both type of barriers, namely the internal qubit and the field diffusion barriers. In Appendix B we analytically calculate the energy poles that arise through the above described method. In the lines that follow we give an example of such calculation, concerning the poles of the unperturbed quantum well meaning region L.

Region L contributes with the pole term:

$$Pole_n^L \sim \left\{ \tilde{\mathcal{G}}_{b,n} \operatorname{Re} \tilde{\mathcal{G}}_{b,n} \right\}^{-1} \quad (17)$$

The poles of the fractional term arise naturally from the condition $\operatorname{Re} \tilde{\mathcal{G}}_b = 0$, which can be equivalently written as

$$\int_a^b k(y) dy = n\pi + \pi/2 \quad (18)$$

Assuming a parabolic type of potential well, as depicted by Figure 2, meaning a function of the form $V(y) = \kappa(y - y_o)^2$, where $\kappa = \frac{2m\pi^2}{T^2}$ with T being the period of classical oscillations and y_o corresponds to the bottom of the well, we can actually calculate the integral in (18) and find the energy poles as

$$E_n = \left(n + \frac{1}{2} \right) \hbar \omega \quad (19)$$

which are the exact eigenvalues of the harmonic potential. Giving another example we can assume a rectangular potential well of infinite walls, which is approximately true as long as we can assure that the internal barrier is much higher than the lower eigenstate of the well. Then we would have instead of (10) the following:

$$\Upsilon^L = -2i \frac{\operatorname{Im} \tilde{\mathcal{G}}_{r_1}^{\pi/4}}{\tilde{\mathcal{G}}_{r_2}^{\pi/4}} + \frac{2 \operatorname{Im} \tilde{\mathcal{G}}_{r_1}^{\pi/4} \operatorname{Im} \tilde{\mathcal{G}}_{r_2}^{\pi/4}}{\tilde{\mathcal{G}}_b \operatorname{Im} \tilde{\mathcal{G}}_b} \quad (20)$$

and consequently

$$\int_a^b k(y)dy = n\pi \Rightarrow \frac{\sqrt{2m}}{\hbar^2} \int_a^b \sqrt{E_n} dy = n\pi \Rightarrow E_n = n^2 \frac{\pi^2 \hbar^2}{2m(b-a)^2} \quad (21)$$

which of course are the exact eigenvalues of a particle in a box. Thus, the pole term of (17) reveals the eigenvalues of the isolated unperturbed potential well.

According to Appendix B the energy eigenvalues for the rest region amplitudes go as following:

a) Regions L and \bar{x} contribute with the perturbed eigenvalues

$$Z_n^{L,\bar{x}} = E_n - \bar{\xi}_{b,n}^{-2} \left\{ d^{E_n} \bar{\xi}(b) \right\} \left(2\sqrt{2} \left\{ d^{E_n} \bar{g}(b) \right\} \right)^{-2} - i \left(d^{E_n} \bar{g}(b) \right)^{-1} \frac{\bar{\xi}_{b,n}^2}{4} \quad (22)$$

where the subscript n denotes calculation on the eigenvalue E_n and where the symbol d^{E_n} denotes derivation with respect to the eigenvalue E_n .

b) Regions L, \bar{x} and R contribute with the perturbed eigenvalues

$$Z_n^{L,\bar{x},R} = E_n - \frac{\left\{ \mp \frac{\bar{\xi}_{b,n}}{2} \left\{ - \left\{ d^{E_n} \bar{g}(b) \right\} \left(1 - \frac{\bar{\xi}_{b,n}^2}{4} \right) \pm \left\{ d^{E_n} \bar{\xi}(b) \right\} \frac{\bar{\xi}_{b,n}}{2} \right\} \right.}{\left. \left\{ - i \frac{\bar{\xi}_{b,n}}{2} \left\{ - \left\{ d^{E_n} \bar{g}(b) \right\} \frac{\bar{\xi}_{b,n}}{2} \left(1 - \frac{\bar{\xi}_{b,n}^2}{4} \right) \pm \left\{ d^{E_n} \bar{\xi}(b) \right\} \frac{\bar{\xi}_{b,n}^2}{4} + \left\{ d^{E_n} \bar{\xi}(b) \right\} \bar{\xi}_{b,n}^2 \mp \left\{ \left\{ d^{E_n} \bar{g}(b) \right\} \right\} \right\} \right\}} \left\{ - \left\{ d^{E_n} \bar{g}(b) \right\} \left(1 - \frac{\bar{\xi}_{b,n}^2}{4} \right) \pm \left\{ d^{E_n} \bar{\xi}(b) \right\} \frac{\bar{\xi}_{b,n}}{2} \right\}^2 + \frac{\bar{\xi}_{b,n}}{2} \left\{ \left\{ d^{E_n} \bar{\xi}(b) \right\} \bar{\xi}_{b,n} \mp \left\{ \left\{ d^{E_n} \bar{g}(b) \right\} \right\} \right\}^2 \right.} \quad (23)$$

c) Regions L, \bar{x} , R, \bar{x} contribute with the perturbed eigenvalues

$$Z_n^{L,\bar{x},R,\bar{x}} = E_n - \frac{\left\{ \mp 2\bar{\xi}_{b,n} \left\{ \left\{ d^{E_n} \bar{g}(b) \right\} \left(4 - \bar{\xi}_{b,n}^2 \right) \pm 2\bar{\xi}_{b,n}^2 \left\{ d^{E_n} \bar{\xi}(b) \right\} \right\} + 2\bar{\xi}_{b,n}^4 \left\{ \left\{ d^{E_n} \bar{\xi}(b) \right\} \mp \bar{\xi}_{b,n} \left\{ d^{E_n} \bar{g}(b) \right\} - 2 \frac{\left\{ d^{E_n} \bar{g}(b) \right\} \bar{\gamma}_{d,n}^2}{\left(\bar{\gamma}_{d,n} \bar{\xi}_{b,n} \right)^2 - \bar{\xi}_{b,n}^4} \right\} \right.}{\left. \left\{ \left\{ d^{E_n} \bar{g}(b) \right\} \left(4 - \bar{\xi}_{b,n}^2 \right) \pm 2\bar{\xi}_{b,n} \left\{ d^{E_n} \bar{\xi}(b) \right\} \right\}^2 + \left\{ 2\bar{\xi}_{b,n}^2 \left\{ \left\{ d^{E_n} \bar{\xi}(b) \right\} \mp \bar{\xi}_{b,n}^{-1} \left\{ d^{E_n} \bar{g}(b) \right\} - 2 \frac{\left\{ d^{E_n} \bar{g}(b) \right\} \bar{\gamma}_{d,n}^2}{\left(\bar{\gamma}_{d,n} \bar{\xi}_{b,n} \right)^2 - \bar{\xi}_{b,n}^4} \right\} \right\}^2 \right.}$$

$$+ i \frac{\left\{ \mp 4\bar{\xi}_{b,n}^3 \left(\frac{1}{2} \left\{ d^{E_n} \bar{\xi}(b) \right\} \mp \frac{\bar{\xi}_{b,n}}{4} \left\{ d^{E_n} \bar{g}(b) \right\} \pm \left\{ d^{E_n} \bar{g}(b) \right\} \frac{\bar{\gamma}_{d,n}^2 \bar{\xi}_{b,n}^{-1}}{\bar{\gamma}_{d,n}^2 - \bar{\xi}_{b,n}^2} \right) \right\}}{\left\{ \left\{ d^{E_n} \bar{g}(b) \right\} \left(4 - \bar{\xi}_{b,n}^2 \right) \pm 2\bar{\xi}_{b,n} \left\{ d^{E_n} \bar{\xi}(b) \right\} \right\}^2 + \left\{ 2\bar{\xi}_{b,n}^2 \left\{ \left\{ d^{E_n} \bar{\xi}(b) \right\} \mp \bar{\xi}_{b,n}^{-1} \left\{ d^{E_n} \bar{g}(b) \right\} - 2 \frac{\left\{ d^{E_n} \bar{g}(b) \right\} \bar{\gamma}_{d,n}^2}{\left(\bar{\gamma}_{d,n} \bar{\xi}_{b,n} \right)^2 - \bar{\xi}_{b,n}^4} \right\} \right\}^2} \quad (24)$$

d) finally regions $L, \bar{\times}, R, \bar{\times}$ and $\bar{\times}$ contribute with the perturbed eigenvalues

$$\begin{aligned}
 Z_n^{L, \bar{\times}, R, \bar{\times}, \bar{\times}} = E_n - & \left\{ \left(\mp 2 \frac{\bar{\xi}_{b,n}^2 - \bar{\delta}_{a,n}^2}{4} \right) \left\{ d^{E_s} \bar{g}(b) \left(4 + \frac{\bar{\xi}_{b,n}^2 - \bar{\delta}_{a,n}^2}{4} \right) - \frac{\bar{\delta}_{a,n}^2}{2} \{ d^{E_s} \bar{\delta}(a) \} \pm 2 \bar{\xi}_{b,n} \{ d^{E_s} \bar{\xi}(b) \} \right\} \right. \\
 & \left. + \left(-2 \frac{\bar{\xi}_{b,n}^2 - \bar{\delta}_{a,n}^2}{4} \right) \left\{ 2 \bar{\xi}_{b,n}^2 \left(\{ d^{E_s} \bar{\xi}(b) \} \mp \bar{\xi}_{b,n}^{-1} \{ d^{E_s} \bar{g}(b) \} \pm 2 \{ d^{E_s} \bar{g}(b) \} \frac{\bar{\xi}_{b,n}^{-1} \bar{\gamma}_{d,n}^2}{\bar{\gamma}_{d,n}^2 - \bar{\xi}_{b,n}^2} \right) - \frac{\bar{\delta}_{a,n}^2}{2} \left(\frac{1}{2} \{ d^{E_s} \bar{g}(b) \} + \{ d^{E_s} \bar{\delta}(a) \} \right) \right\} \right\} \\
 & \left\{ \left\{ d^{E_s} \bar{g}(b) \left(-4 + \frac{\bar{\xi}_{b,n}^2 - \bar{\delta}_{a,n}^2}{4} \right) \pm 2 \bar{\xi}_{b,n} \{ d^{E_s} \bar{\xi}(b) \} - \frac{\bar{\delta}_{a,n}^2}{2} \{ d^{E_s} \bar{\delta}(a) \} \right\}^2 + \right. \\
 & \left. \left\{ 2 \bar{\xi}_{b,n}^2 \left(\{ d^{E_s} \bar{\xi}(b) \} \mp \bar{\xi}_{b,n}^{-1} \{ d^{E_s} \bar{g}(b) \} \pm 2 \{ d^{E_s} \bar{g}(b) \} \frac{\bar{\xi}_{b,n}^{-1} \bar{\gamma}_{d,n}^2}{\bar{\gamma}_{d,n}^2 - \bar{\xi}_{b,n}^2} \right) - \frac{\bar{\delta}_{a,n}^2}{2} \left(\frac{1}{2} \{ d^{E_s} \bar{g}(b) \} + \{ d^{E_s} \bar{\delta}(a) \} \right) \right\}^2 \right\} \\
 & + i \left\{ \left(\mp 2 e^{-\phi(\lambda_s)} - \frac{e^{-2\phi_s(\nu)}}{4} \right) \left\{ 2 e^{-2\phi_s(\lambda)} \left(\{ d^{E_s} \bar{\xi}(b) \} \mp e^{\phi_s(\lambda)} \{ d^{E_s} \bar{g}(b) \} \pm 2 \{ d^{E_s} \bar{g}(b) \} \frac{e^{-2\gamma_s(\nu)+\phi_s(\lambda)}}{e^{-2\gamma_s(\nu)} - e^{-2\phi_s(\lambda)}} \right) - \frac{\bar{\delta}_{a,n}^2}{2} \left(\frac{1}{2} \{ d^{E_s} \bar{g}(b) \} + \{ d^{E_s} \bar{\delta}(a) \} \right) \right\} + \right. \\
 & \left. \left(e^{-\phi(\lambda_s)} + \frac{\bar{\delta}_{a,n}^2}{4} \right) \left\{ \{ d^{E_s} \bar{g}(b) \} \left(-4 + \frac{\bar{\xi}_{b,n}^2 - \bar{\delta}_{a,n}^2}{4} \right) \pm 2 e^{-\phi_s(\lambda)} \{ d^{E_s} \bar{\xi}(b) \} - \frac{\bar{\delta}_{a,n}^2}{2} \{ d^{E_s} \bar{\delta}(a) \} \right\} \right. \\
 & \left. \left\{ \left\{ d^{E_s} \bar{g}(b) \left(-4 + \frac{\bar{\xi}_{b,n}^2 - \bar{\delta}_{a,n}^2}{4} \right) \pm 2 \bar{\xi}_{b,n} \{ d^{E_s} \bar{\xi}(b) \} - \frac{\bar{\delta}_{a,n}^2}{2} \{ d^{E_s} \bar{\delta}(a) \} \right\}^2 + \right. \right. \\
 & \left. \left. \left\{ 2 \bar{\xi}_{b,n}^2 \left(\{ d^{E_s} \bar{\xi}(b) \} \mp \bar{\xi}_{b,n}^{-1} \{ d^{E_s} \bar{g}(b) \} \pm 2 \{ d^{E_s} \bar{g}(b) \} \frac{\bar{\xi}_{b,n}^{-1} \bar{\gamma}_{d,n}^2}{\bar{\gamma}_{d,n}^2 - \bar{\xi}_{b,n}^2} \right) - \frac{\bar{\delta}_{a,n}^2}{2} \left(\frac{1}{2} \{ d^{E_s} \bar{g}(b) \} + \{ d^{E_s} \bar{\delta}(a) \} \right) \right\}^2 \right\} \right\}
 \end{aligned} \tag{25}$$

FIELD INDUCED DYNAMICS OF A QUBIT STATE

The time evolution of a qubit state in a double well structure, as this is induced by the presence of two independent field barriers depicted by Figure 2, concerns the alteration of the Hadamard Time, as well as the appearance of the exponential decay of the initial state into the continuum. As we have already seen the spectrum turns to be complex taking the following form for the lowest state: $E_o + \delta E_o - i \frac{\Gamma_o}{2}$. As far as the real part is concerned, the result is the splitting of the E_o which is the lowest energy of the unperturbed wells, into two new states, with energies equal to

$$E_S = E_o + \delta E_o^s, \quad E_A = E_o + \delta E_o^a \tag{26}$$

and then the Hadamard Time is given according to (16) as

$$T_{Hd/f} = \frac{h}{4(\delta E_o^a - \delta E_o^s)} \tag{27}$$

where the subscript f generally denotes the presence of a field barrier.

In the absence of the field barriers the WKB approximation is obtained as [24,26]

$$T_{Hd/WKB} = \frac{\pi^2}{2\omega\widehat{\xi}_{b,o}} \quad (28)$$

where ω is the frequency of the classical periodic motion between turning points a and b corresponding to energy E_o . The above result in (26) is obtained using the linear connection formulae. In the lines that follow we calculate the Hadamard Time separately for the cases of i) the unperturbed DWP, ii) the double well plus field barrier f_1 and iii) the double well plus both field barriers $+f_1$ and $+f_2$ depicted by Figure 2.

i) The case of the Unperturbed Double Well Potential:

According to (23) the real parts of the doublet splitting, read

$$E_o^{L,\bar{x},R} = E_o - \frac{\mp \frac{\widehat{\xi}_{b,o}}{2} \left\{ -\{d^{E_o} \bar{\mathfrak{g}}(b)\} \left(1 - \frac{\widehat{\xi}_{b,o}^2}{4} \right) \pm \{d^{E_o} \bar{\xi}(b)\} \frac{\widehat{\xi}_{b,o}}{2} \right\}}{\left\{ -\{d^{E_o} \bar{\mathfrak{g}}(b)\} \left(1 - \frac{\widehat{\xi}_{b,o}^2}{4} \right) \pm \{d^{E_o} \bar{\xi}(b)\} \frac{\widehat{\xi}_{b,o}}{2} \right\}^2 + \frac{\widehat{\xi}_{b,o}}{2} \left\{ \{d^{E_o} \bar{\xi}(b)\} \widehat{\xi}_{b,o} \mp \left(\{d^{E_o} \bar{\mathfrak{g}}(b)\} \right) \right\}^2} \quad (29)$$

Thus the Hadamard Time is given as:

$$T_{Hd}^{L,\bar{x},R} = T_{Hd/WKB} \left\{ \frac{\frac{1}{2} \left\{ \left(1 - \frac{\widehat{\xi}_{b,o}^2}{4} \right) - \text{sim}(\bar{\xi}, \bar{\mathfrak{g}}) \frac{\widehat{\xi}_{b,o}}{2} \right\}}{\left\{ \left(1 - \frac{\widehat{\xi}_{b,o}^2}{4} \right) + \text{sim}(\bar{\xi}, \bar{\mathfrak{g}}) \frac{\widehat{\xi}_{b,o}}{2} \right\}^2 + \frac{\widehat{\xi}_{b,o}}{2} \left\{ \text{sim}(\bar{\xi}, \bar{\mathfrak{g}}) \widehat{\xi}_{b,o} + 1 \right\}^2} + \frac{1}{2} \left\{ \left(1 - \frac{\widehat{\xi}_{b,o}^2}{4} \right) + \text{sim}(\bar{\xi}, \bar{\mathfrak{g}}) \frac{\widehat{\xi}_{b,o}}{2} \right\}}{\left\{ \left(1 - \frac{\widehat{\xi}_{b,o}^2}{4} \right) - \text{sim}(\bar{\xi}, \bar{\mathfrak{g}}) \frac{\widehat{\xi}_{b,o}}{2} \right\}^2 + \frac{\widehat{\xi}_{b,o}}{2} \left\{ \text{sim}(\bar{\xi}, \bar{\mathfrak{g}}) \widehat{\xi}_{b,o} - 1 \right\}^2} \right\}^{-1} \quad (30)$$

which of course goes far beyond the WKB expression. In fact, as can clearly be seen, eq. (30) reduces to (28) by keeping only the dominant terms (omitting terms like $e^{-2\phi_o(\lambda)}$ or smaller), and taking the barrier to be energy independent, meaning taking $\{d^{E_o} \bar{\xi}(b)\} = 0$, for a small energy area around E_o where the splitting takes place.

Thus we are motivated to further explore the energy dependence of the Hadamard Time. For this, we introduced in (30) quantity

$$\{d^{E_0} \widehat{\xi}(b)\} / \{d^{E_0} \check{\mathcal{G}}(b)\} \equiv \text{sim}(\widehat{\xi}, \check{\mathcal{G}}) \quad (31)$$

defined as the “shape similarity factor” between the barrier and the well, given as the ratio of the change in barrier magnitude to the change in well magnitude, as energy increases, some kind of $\widehat{\xi}(b)$ derivative with respect to $\check{\mathcal{G}}(b)$. It is easily understood that the above quantity is negative since $\check{\mathcal{G}}(b)$ increases with the increment of the energy while $\widehat{\xi}(b)$ decreases. The above are depicted by Figure 4 that follows.

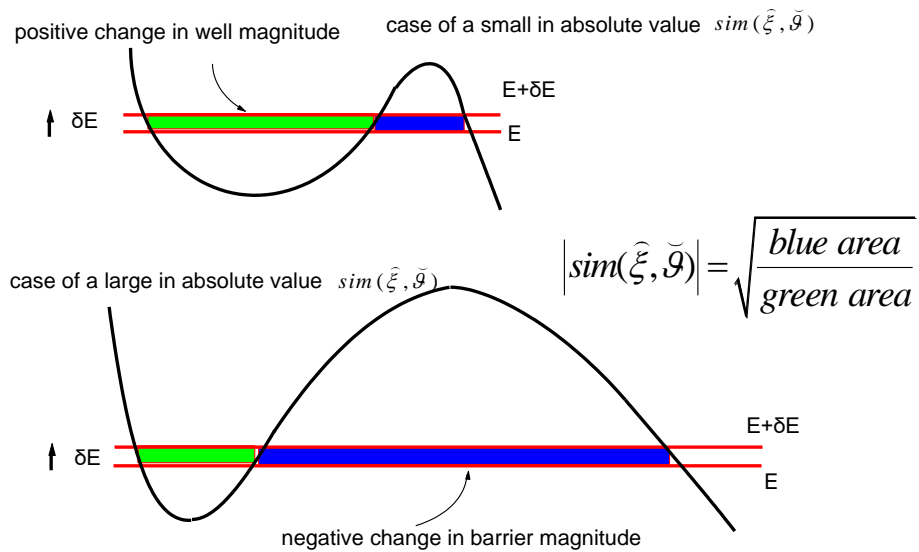


FIGURE 4. The variation of the shape similarity factor $\text{sim}(\widehat{\xi}, \check{\mathcal{G}})$ for two different cases of the potential barrier shape, relative to the one of the potential well. Note that the blue colour denotes a negative change in the barrier magnitude as energy increases (shorter barrier) while the green colour a positive change in the well magnitude (deeper well).

In Figure 5 that follows we depict Hadamard Time as a function of the similarity factor for two different values of the qubit barrier, employing (30).

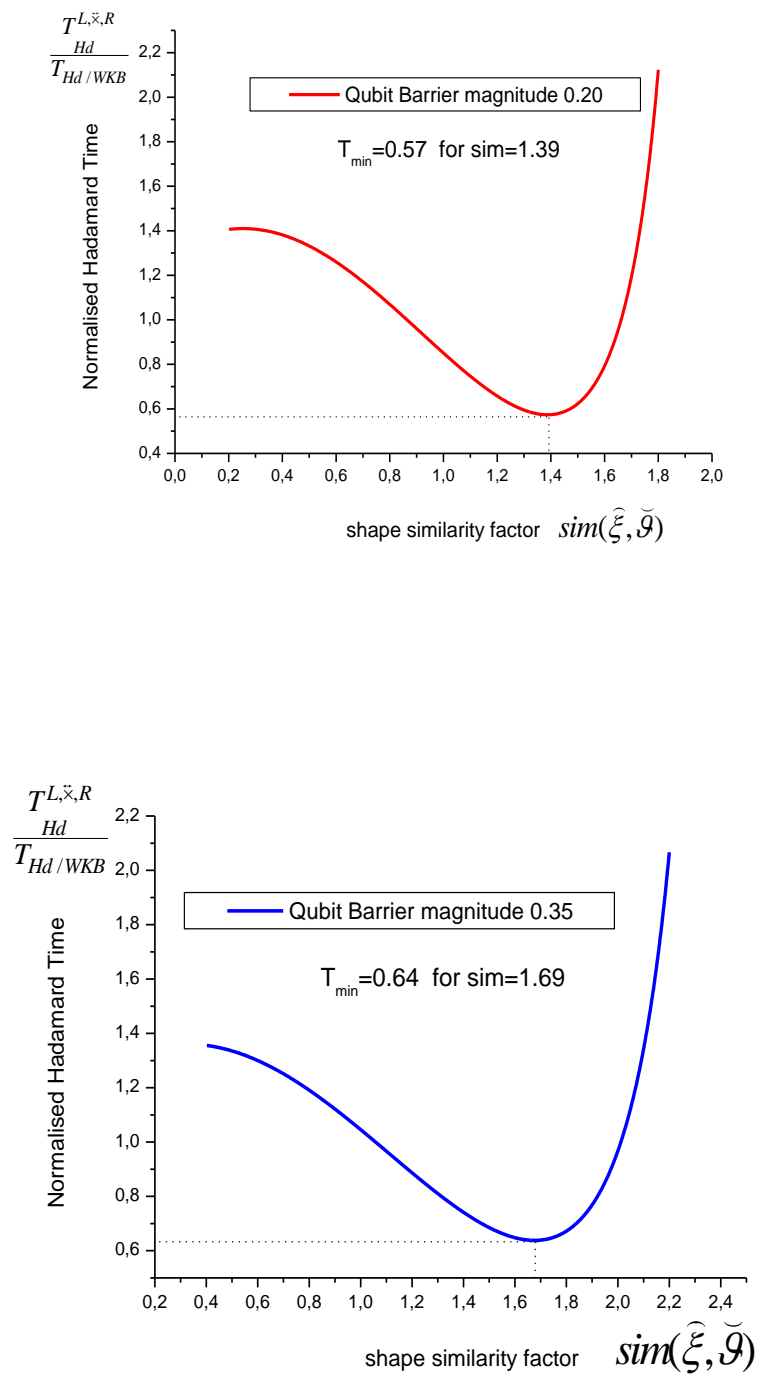


FIGURE 5. The variation of the Hadamard Time, (normalised to the WKB expression), as a function of the similarity factor $sim(\tilde{\xi}, \tilde{\mathcal{G}})$ which relates the change of the field magnitude to the change of the well magnitude with energy increment, for two different values of the qubit barrier magnitude. For each case the Hadamard Time becomes minimum for a certain value of the similarity factor $sim(\tilde{\xi}, \tilde{\mathcal{G}})$.

ii) Field barrier f_1 active and field barrier f_2 inactive

According to (B-9) of Appendix B the real parts of the energy splitting, read

$$E_o^{L,\bar{x},R,\bar{x}} = E_o - \frac{\left\{ \mp 2\widehat{\xi}_{b,o} \left\{ \left\{ d^{E_o} \bar{g}(b) \right\} \left(4 - \widehat{\xi}_{b,o}^2 \right) \pm 2\widehat{\xi}_{b,o} \left\{ d^{E_o} \bar{\xi}(b) \right\} \right\} + 2\widehat{\xi}_{b,o}^4 \left(\left\{ d^{E_o} \bar{\xi}(b) \right\} \mp \widehat{\xi}_{b,o} \left\{ d^{E_o} \bar{g}(b) \right\} - 2 \frac{\left\{ d^{E_o} \bar{g}(b) \right\} \widehat{\gamma}_{d,o}^2}{\left(\widehat{\gamma}_{d,o} \widehat{\xi}_{b,o} \right)^2 - \widehat{\xi}_{b,o}^4} \right) \right\}}{\left\{ \left\{ d^{E_o} \bar{g}(b) \right\} \left(4 - \widehat{\xi}_{b,o}^2 \right) \pm 2\widehat{\xi}_{b,o} \left\{ d^{E_o} \bar{\xi}(b) \right\} \right\}^2 + \left\{ 2\widehat{\xi}_{b,o}^2 \left(\left\{ d^{E_o} \bar{\xi}(b) \right\} \mp \widehat{\xi}_{b,o}^{-1} \left\{ d^{E_o} \bar{g}(b) \right\} - 2 \frac{\left\{ d^{E_o} \bar{g}(b) \right\} \widehat{\gamma}_{d,o}^2}{\left(\widehat{\gamma}_{d,o} \widehat{\xi}_{b,o} \right)^2 - \widehat{\xi}_{b,o}^4} \right) \right\}^2} \quad (32)$$

For the present purpose we currently disregard the energy dependence of the field barrier and write the real parts of the energy splitting as follows

$$E_o^{L,\bar{x},R,\bar{x}} = E_o - \frac{\left\{ \mp 8\widehat{\xi}_{b,o} \mp 2\widehat{\xi}_{b,o}^3 - 4 \left(\frac{\widehat{\gamma}_{d,o}^2}{\widehat{\gamma}_{d,o}^2 \widehat{\xi}_{b,o}^{-2} - 1} \right) \right\}}{\left\{ 16 \left\{ d^{E_o} \bar{g}(b) \right\} \right\} \left\{ 1 + \left(\frac{\widehat{\gamma}_{d,o}^2}{\widehat{\gamma}_{d,o}^2 - \widehat{\xi}_{b,o}^2} \right)^2 \right\}} \quad (33)$$

Thus the Hadamard Time is given as:

$$T_{Hd}^{f_1} = T_{Hd/WKB} \left(1 + \frac{\widehat{\xi}_{b,o}^2}{4} \right)^{-1} \left\{ 1 + \left(\frac{\widehat{\gamma}_{d,o}^2}{\widehat{\gamma}_{d,o}^2 - \widehat{\xi}_{b,o}^2} \right)^2 \right\} \Rightarrow \quad (34)$$

$$\frac{T_{Hd}^{f_1}}{T_{Hd/WKB}} = \left(1 + \frac{\widehat{\xi}_{b,o}^2}{4} \right)^{-1} \left\{ 1 + \left(\frac{e^{-2\delta m}}{e^{-2\delta m} - 1} \right)^2 \right\}$$

where we have introduced the dimensionless quantity

$$\delta m = \ln \left(\widehat{\xi}_b / \widehat{\gamma}_d \right) \quad (35)$$

as a measure of the difference in magnitude between the qubit and the field barrier f_1 .

In Figure 6 that follows, we depict the variation of the ratio $T_{Hd}^{f_1} / T_{Hd/WKB}$ with quantity δm . It is clearly seen that as δm increases, the normalised Hadamard Time tends to unity, since then the field barrier becomes almost impenetrable and the Hadamard Time coincides with the one from the WKB approximation. On the contrary when the difference in magnitude between the qubit and the field barrier becomes negligible, Hadamard Time increases a lot.

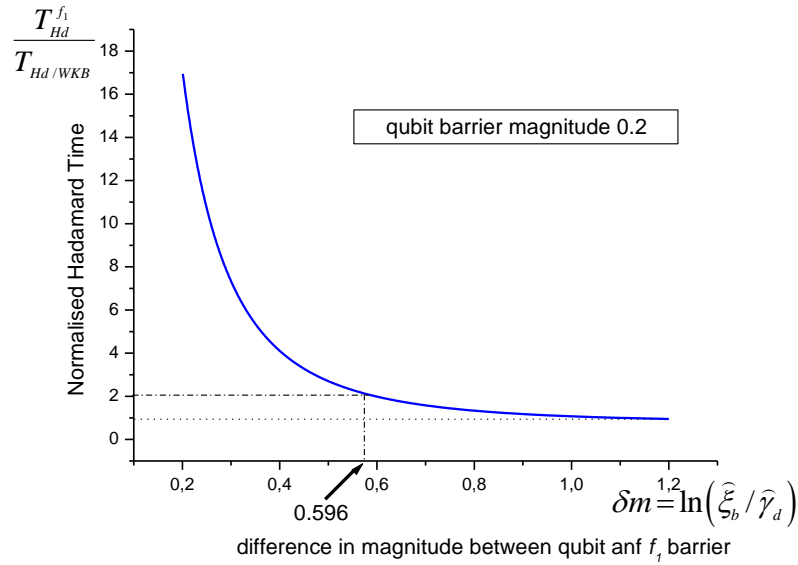


FIGURE 6. The normalised Hadamard Time as a function of the difference in magnitude between the field and the qubit barrier. Hadamard Time tends to the WKB expression as the difference in magnitude increases and reaches a value twice the WKB one, for a difference in magnitude of the two barriers equal to 0.596.

iii) Both field barriers f_1 and f_2 active.

According to (B-12) the real parts of the energy splitting, read

$$E_o^{L,\bar{x},R,\bar{x},\bar{x}} = E_o - \frac{\left\{ \begin{aligned} &\left(\mp 2\bar{\xi}_{b,o} - \frac{\bar{\delta}_{a,o}^2}{4} \right) \left\{ d^{E_o} \bar{g}(b) \left(4 + \bar{\xi}_{b,o}^2 - \frac{\bar{\delta}_{a,o}^2}{4} \right) - \frac{\bar{\delta}_{a,o}^2}{2} \{ d^{E_o} \bar{\delta}(a) \} \pm 2\bar{\xi}_{b,o} \{ d^{E_o} \bar{\xi}(b) \} \right\} \\ &+ \left(-2\bar{\xi}_{b,o}^2 - \frac{\bar{\delta}_{a,o}^2}{4} \right) \left\{ 2\bar{\xi}_{b,o}^2 \left(\{ d^{E_o} \bar{\xi}(b) \} \mp \bar{\xi}_{b,o}^{-1} \{ d^{E_o} \bar{g}(b) \} \pm 2 \{ d^{E_o} \bar{g}(b) \} \frac{\bar{\xi}_{b,o}^{-1} \bar{\gamma}_{d,o}^2}{\bar{\gamma}_{d,o}^2 - \bar{\xi}_{b,o}^2} \right) - \frac{\bar{\delta}_{a,o}^2}{2} \left(\frac{1}{2} \{ d^{E_o} \bar{g}(b) \} + \{ d^{E_o} \bar{\delta}(a) \} \right) \right\} \end{aligned} \right\}}{\left\{ \begin{aligned} &\left\{ \{ d^{E_o} \bar{g}(b) \} \left(-4 + \bar{\xi}_{b,o}^2 - \frac{\bar{\delta}_{a,o}^2}{4} \right) \pm 2\bar{\xi}_{b,o} \{ d^{E_o} \bar{\xi}(b) \} - \frac{\bar{\delta}_{a,o}^2}{2} \{ d^{E_o} \bar{\delta}(a) \} \right\}^2 + \\ &\left\{ 2\bar{\xi}_{b,o}^2 \left(\{ d^{E_o} \bar{\xi}(b) \} \mp \bar{\xi}_{b,o}^{-1} \{ d^{E_o} \bar{g}(b) \} \pm 2 \{ d^{E_o} \bar{g}(b) \} \frac{\bar{\xi}_{b,o}^{-1} \bar{\gamma}_{d,o}^2}{\bar{\gamma}_{d,o}^2 - \bar{\xi}_{b,o}^2} \right) - \frac{\bar{\delta}_{a,o}^2}{2} \left(\frac{1}{2} \{ d^{E_o} \bar{g}(b) \} + \{ d^{E_o} \bar{\delta}(a) \} \right) \right\}^2 \end{aligned} \right\}} \quad (36)$$

Thus, we get for the Hadamard Time the following expression:

$$\frac{T_{Hd}^{f_1, f_2}}{T_{Hd/WKB}} = \frac{T_{Hd}^1 T_{Hd}^2}{T_{Hd/WKB} (T_{Hd}^1 - T_{Hd}^2)} \quad (37)$$

with

$$T_{Ha}^{2(top\ sign)} = T_{Ha/WKB}^{1(down\ sign)} \left(\frac{\left(-4 \pm 2 \operatorname{sim}(\tilde{\xi}, \tilde{\vartheta}) \tilde{\xi}_{b,o} - \operatorname{sim}(\tilde{\delta}, \tilde{\vartheta}) \frac{\tilde{\delta}_{a,o}^2}{2} \right)^2 + \left(\mp 2 \tilde{\xi}_{b,o} \left(1 - 2 \frac{e^{2\delta m}}{e^{2\delta m} - 1} \right) \right)^2}{\left\{ \left(-4 \tilde{\xi}_{b,o} - \frac{\tilde{\delta}_{a,o}^2}{2} \right) \left(\mp 2 \pm 4 \frac{e^{2\delta m}}{e^{2\delta m} - 1} \right) - \frac{5}{4} \tilde{\xi}_{b,o}^{-1} \tilde{\delta}_{a,o}^2 \mp 8 \right\} + \left\{ \operatorname{sim}(\tilde{\xi}, \tilde{\vartheta}) \left(-4 \tilde{\xi}_{b,o} + 2 \tilde{\xi}_{b,o} \left(-2 \tilde{\xi}_{b,o}^2 - \frac{\tilde{\delta}_{a,o}^2}{4} \right) \right) \right\} + \left\{ \operatorname{sim}(\tilde{\delta}, \tilde{\vartheta}) \left(\pm \tilde{\delta}_{a,o}^2 + \frac{\tilde{\delta}_{a,o}^2}{2} \left(2 \tilde{\xi}_{b,o} - \frac{\tilde{\xi}_{b,o}^{-1} \tilde{\delta}_{a,o}^2}{4} \right) \right) \right\}} \right) \quad (38)$$

In Table 3 that follows we include the values of various parameters that were employed in (38), as these were taken from our previous results.

Parameter	Value
Qubit barrier strength $\varphi(\lambda)$ (Figure 5)	0.20 / 0.35
Difference in strength $\delta m = \ln(\tilde{\xi}_b / \tilde{\gamma}_d)$ for 200% of the WKB value of the Hadamard Time (Figure 6)	0.596 / 0.693
$\operatorname{sim}(\tilde{\xi}, \tilde{\vartheta})$: similarity factor for minimum value of the normalized Hadamard Time in (Figure 5)	1.39 / 1.69
δ field barrier magnitude	0.35

TABLE 3. The values of the parameters used in (38) for producing Figure 7

Thus we produce Figure 7 that follows, where the variation of the normalised Hadamard Time as a function of the similarity factor $\operatorname{sim}(\tilde{\delta}, \tilde{\vartheta})$ is depicted.

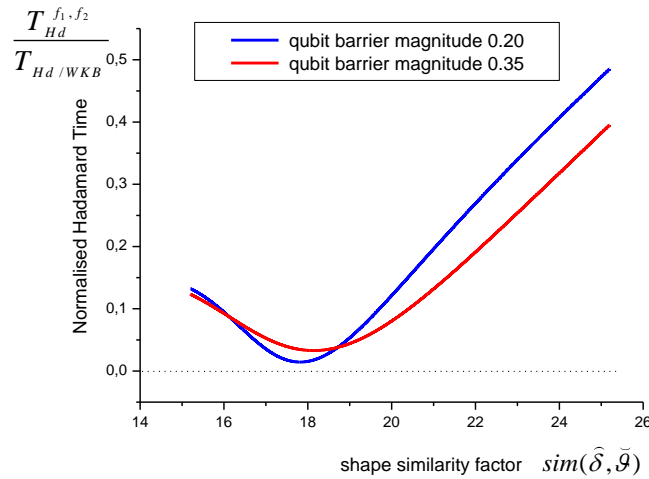


FIGURE 7. The variation of the normalised Hadamard Time as a function of the similarity factor $sim(\tilde{\delta}, \tilde{\mathcal{G}})$ which relates the change of the δ field barrier magnitude to the change of the well magnitude with energy increment, for two different values of the qubit barrier magnitude.

As far as the imaginary part is concerned, we should point out that this contributes to the exponential decay rate of the initial state. This can be seen by taking the Fourier transform of the Breit-Wigner or Lorentzian decay amplitude

$$Gr(E) = \frac{i}{E - \left(E_o + \delta E_o - i \frac{\Gamma_o}{2} \right)} \quad (39)$$

and extending the spectrum to the full real axis $-\infty < E < \infty$ instead of being bounded from below $0 \leq E < \infty$ (“Fermi’s approximation”). The time evolution of the decaying state is then given by

$$\Psi(t) = e^{-i(E_o + \delta E_o)t/\hbar} e^{-\Gamma_o t/2\hbar} \Psi(0) \quad (40)$$

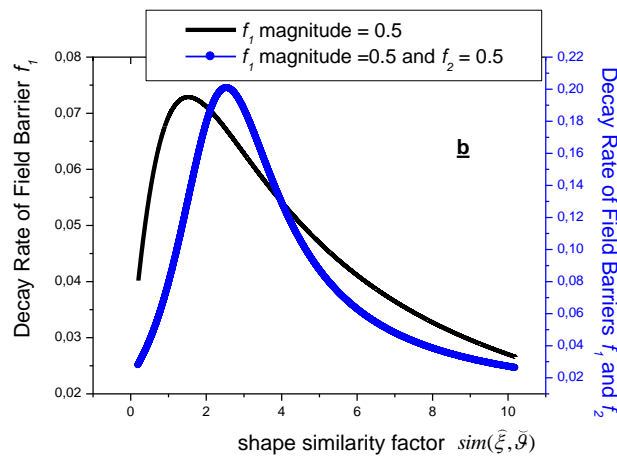
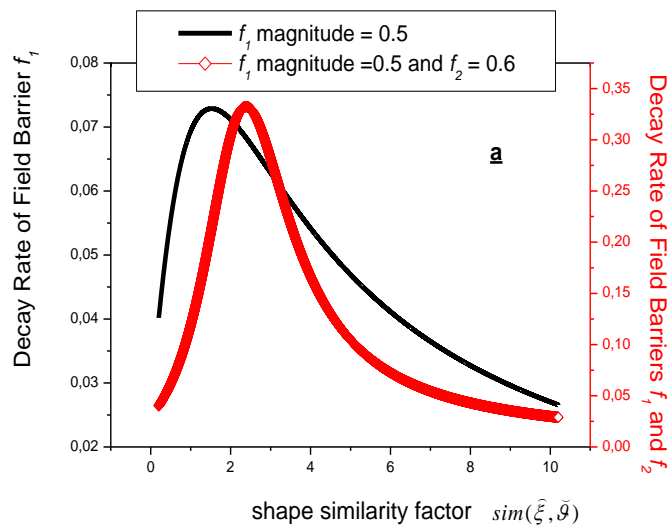
Thus the survival probability of the initial state is given as

$$P(t) \sim e^{-\Gamma_o t/\hbar} \quad (41)$$

and this is called exponential decay. The decoherence of a quantum superposition state due to its interaction with the environment leads to an exponential decay law, [65,66]. Thus, \hbar/Γ_o is a meter of the qubit’s decoherence time, meaning the time interval that the coherent superposition state survives. However if we do not necessarily extend the spectrum we will also find non exponential contributions for both small and large times. As far as the region of large times is concerned the non exponential contribution dominates the system’s evolution and takes the following form, [64],

$$P(t) \sim \left\{ \left\{ (E_o + \delta E_o)^2 + \frac{\Gamma_o^2}{4} \right\} t^2 \right\}^{-1} \tag{42}$$

In Figure 8 that follows we depict exponential decay rates $\Gamma_o^{L,\tilde{x},R,\tilde{x}}$ and $\Gamma_o^{L,\tilde{x},R,\tilde{x},\tilde{x}}$ which are twice the imaginary parts of (B-9) and (B-12) respectively, as a function of the similarity factor $sim(\tilde{\xi}, \tilde{\vartheta})$, for the parameter values contained in Table 5. In addition we extract the value of 18.2 for the similarity factor $sim(\tilde{\delta}, \tilde{\vartheta})$, taken from Figure 7, which makes the corresponding Hadamard Time a minimum.



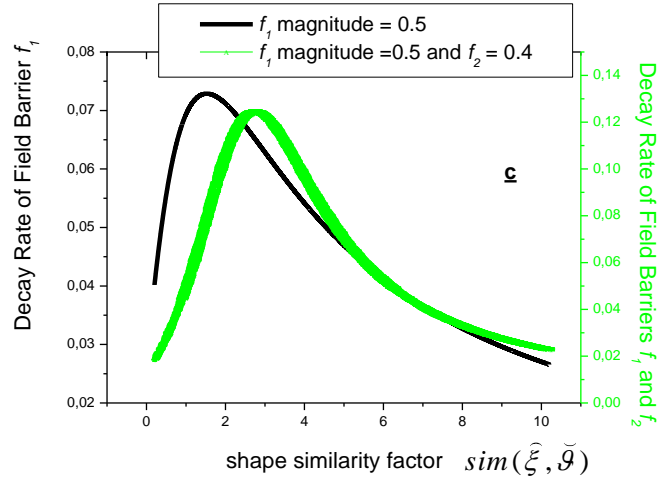


FIGURE 8. Comparison of the exponential decay rate for barrier field f_1 only active and both barrier fields f_1 and f_2 active, as a function of the similarity factor $\text{sim}(\hat{\xi}, \tilde{\theta})$, for three different cases as far as the relative magnitude of the field barriers is concerned: a) $f_1 < f_2$ b) $f_1 = f_2$, c) $f_1 > f_2$. Note that the two rates come in different orders of magnitude.

CONCLUDING REMARKS

In this paper, we studied the dynamics of a positional-based qubit structure as this is induced and controlled by the presence of two independent electrostatic fields. Our attention focused on the Hadamard Time, defined in the present paper as the time needed for the initial state to come in an equally weighted coherent superposition of the two orthogonal qubit states $|0\rangle$ and $|1\rangle$, through the particle's probabilistic appearance in both quantum wells. First, we analytically solved the model providing analytical relations for the system's Green function and energy eigenvalues. Second, we gave analytical expressions for the intrinsic qubit's time needed for oscillation between its orthogonal states and more than this of the time required for decoherence to appear through exponential decay.

In quantum computation, knowledge of the Hadamard Time is significant since it corresponds to the knowledge of the time needed for quantum coherent superposition to appear. The latter makes a substantial difference to quantum computing compared to its classical counterpart and makes quantum calculations much faster and the quantum computational system itself much more capable, [1]. Thus, in order to carry out quantum computations we should, at first, adjust the clock frequency of the computational system to the "frequency" $f = 1/T_{\text{Hd}}$ of series of revivals of the superposition state. One can produce entangled states through such suitably prepared superposition states, [67]. Thus, frequency adjustment is required for quantum cryptography as well. In addition, our computing system gets less complicated since now no Hadamard gate is needed. At the same time, decoherence is unavoidable due to the qubit's interaction with the environment. Decoherence destroys quantum superposition and forces the system to decay. The exponential decay rates that we analytically calculated in the current paper provide a decoherence time scale for the

duration of the computational calculations, maintaining their effectivity and accuracy. Decoherence time should be much longer than the period of revivals of the superposition state, [48]. In addition, the analytic study of the above phenomena through path integral theory provides more insight into the physics of the system.

In particular equation (30) gives the Hadamard Time in the case of the unperturbed or ideally isolated qubit. Clearly our result goes far beyond the WKB expression. But most importantly introduces quantity $sim(\tilde{\xi}, \tilde{\vartheta})$, defined as the similarity factor that relates the shape of the well to the one of the barrier as explained in Figure 4. As far as our knowledge goes this quantity has never before been introduced in the international bibliography. It is some kind of correction to the phase event reflection factors that contribute to the path integral calculation, (see the discussion at the end of the first section). In Figure 5 that follows eq. (30), we have depicted the dependence of the normalized (to the WKB expression) Hadamard Time on the similarity factor $sim(\tilde{\xi}, \tilde{\vartheta})$, for two different values of the qubit barrier magnitude. The Hadamard Time receives a minimum value. Both the minimum and the minimum position are increasing functions of the qubit barrier magnitude. Thus the DWP can be suitably engineered for Hadamard Time to receive its minimum value. The latter is very important since then small variations in the qubit's potential will not alter Hadamard Time and consequently will not change the time scale of computation ensuring stability. Hadamard Time tends to a constant value when the well and the barrier are not shape related, $sim(\tilde{\xi}, \tilde{\vartheta})=0$, but increases unlimited as $sim(\tilde{\xi}, \tilde{\vartheta})$ increases, since then the qubit barrier becomes almost impenetrable.

For the case of the field barrier f_l alone, which permits the interaction of the qubit state with the continuum, eq. (33) describes the dependence of the Hadamard Time on the difference in magnitude of the qubit and the field barrier, with the later expressed through quantity δm defined in (34). In Figure 6 we depict the above mentioned dependence for a qubit barrier magnitude equal to 0.2. It is clearly seen that the Hadamard Time tends to the WKB expression as the difference in magnitude increases, since then the field barrier becomes impenetrable. On the other hand as the magnitude of the field barrier is lowered approaching the one of the qubit barrier, Hadamard Time increases, since then tunnelling is equally preferable by both mechanisms: internal oscillation and external diffusion to the continuum. Giving an example, Hadamard Time becomes twice the WKB expression for a difference in barrier magnitude nearly equal to 0.6. The field barrier magnitude is directly dependent on the field strength imposed on the qubit. Hence a suitably engineered DWP and a suitable applied electrostatic field f_l , including its starting point and slope, uniquely determine the computational time scale.

When both field barriers are active, we are interested not only for the change in Hadamard Time but for the change of the exponential decay rate as well, compared to the case of the field f_l alone. Thus, in Figure 7 we depict the dependence of the Hadamard Time with the factor $sim(\tilde{\delta}, \tilde{\vartheta})$ which relates the change of the δ field barrier magnitude to the change of the well magnitude with energy increment, for two different values of the qubit barrier magnitude. The Hadamard Time becomes minimum for a certain value of the similarity function. Both the minimum value and the minimum position are increasing functions of the qubit barrier magnitude. Quite impressively, the minimum region corresponds to much larger values of the similarity factor compared to the case of the perfectly isolated DWP. Actually, their difference is equal to one order of magnitude. In addition, minimum Hadamard Time becomes much smaller, enabling fast but still stable quantum calculations. Interestingly

enough, the curve corresponding to the larger qubit barrier, is positioned under the smaller qubit barrier curve, after a characteristic value of the similarity factor.

As far as the exponential decay rate is concerned, we compare the case where both field barriers, f_1 and f_2 , are present, with the one where only the field barrier f_1 is active. In Figure 8, we have sketched the decay rate as a function of the similarity factor $sim(\tilde{\xi}, \tilde{\mathcal{G}})$, for the previously mentioned field presences, examining separately three different values of the f_2 magnitude: greater, equal and less than the f_1 magnitude where the latter is assumed to remain constant. In each case the two rates come in different orders of magnitude and their difference is an increasing function of the f_2 barrier magnitude. Hence, the qubit state decays much faster due to the presence of a double field barrier. However, for large values of the similarity factor, the two rates become nearly equal, since then the dominant mechanism is the internal oscillation and not decoherence. Finally, let us assume that f_1 stands for the system interaction with its environment while f_2 electrostatically controls the qubit. Interestingly enough, the case of nearly equal barriers, as is shown in figure 8c, does not speed up the system's decay compared to the situation where control is absent. In other words, we can control the qubit without accelerating its decoherence.

APPENDIX A:

Analytic calculation of the propagation amplitudes beyond Y^L .

i) Transition Amplitude $Y^{L,\tilde{x}}$

This includes propagation inside the classically allowed region of state $|0\rangle$ and the classically forbidden internal barrier \tilde{x} . This will affect the eigenvalues of state $|0\rangle$ which will be naturally perturbed. We use the following symbolism: $Y^{L,\tilde{x}} \equiv \{L \rightleftharpoons_{r_1}^b \tilde{x}\} A_L(b; r_2)$, in order to indicate the fact that we must first alternate region L with the one of the internal barrier, in all possible (infinite) ways between points r_1 and b , and then propagate in all possible ways from point b to r_2 , while staying at region L. So, we must first come to point b which is common for the two regions and this results to $A_L(r_1; b)$. Then we interchange the two regions in all possible ways, starting and ending at turning point b . We finally propagate inside region L, between b and r_2 . According to the above we have:

$$Y^{L,\tilde{x}} = A_L(r_1; b) A_{\tilde{x}}(b; b) \{1 - A_L(b; b) A_{\tilde{x}}(b; b)\}^{-1} A_L(b; r_2) \quad (A-1)$$

Repeating the procedure of the previous paragraph, by substituting the phase event factors and doing the tedious algebra we find:

$$Y^{L,\tilde{x}} = -2 \frac{\text{Im} \tilde{\mathcal{G}}_{r_1}^{\pi/4} \text{Im} \tilde{\mathcal{G}}_{r_2}^{\pi/4}}{\tilde{\mathcal{G}}_b} \left\{ \frac{1}{\text{Re} \tilde{\mathcal{G}}_b} - \frac{1}{\text{Re} \tilde{\mathcal{G}}_b - \frac{\tilde{\mathcal{G}}_b \tilde{\xi}^2}{4 + \tilde{\xi}_b^2}} \right\} \quad (A-2)$$

ii) Transition Amplitude $\Upsilon^{L,\tilde{x},R}$

In this case state $|0\rangle$ not only interacts with the internal barrier but with state $|1\rangle$ as well. It is obvious that we must first come to turning point c , by interchanging in all possible ways the regions of L , \tilde{x} , R , and then interchange the couples (L, \tilde{x}) and (R, \tilde{x}) in all possible ways. Finally we can propagate to point r_2 through the couple (L, \tilde{x}) or by staying entirely at region L . Putting all these together we get

$$\Upsilon^{L,\tilde{x},R} = \{L \rightleftharpoons_{r_1}^c \tilde{x}\} \{q \rightleftharpoons_c^b \tilde{x}\} [1 - \{L \rightleftharpoons_b^c \tilde{x}\} \{R \rightleftharpoons_c^b \tilde{x}\}]^{-1} [\{L \rightleftharpoons_b^{r_2} \tilde{x}\} + A_L(b; r_2)] \quad (\text{A-3})$$

Table A₁ that follows contains the above coupled regions propagation amplitudes as these are calculated in terms of fundamental amplitudes:

Amplitudes for the regions L, \tilde{x}, R	Function of Fundamental Amplitudes
$\{L \rightleftharpoons_{r_1}^c \tilde{x}\}$	$A_L(r_1; b) A_{\tilde{x}}(b; c) \{1 - A_L(b; b) A_{\tilde{x}}(b; b)\}^{-1}$
$\{L \rightleftharpoons_b^c \tilde{x}\}$	$A_L(b; b) A_{\tilde{x}}(b; c) \{1 - A_L(b; b) A_{\tilde{x}}(b; b)\}^{-1}$
$\{L \rightleftharpoons_b^{r_2} \tilde{x}\}$	$A_L(b; b) A_{\tilde{x}}(b; b) [1 - A_L(b; b) A_{\tilde{x}}(b; b)]^{-1} A_L(b; r_2)$
$\{R \rightleftharpoons_c^b \tilde{x}\}$	$A_R(c; c) A_{\tilde{x}}(c; b) \{1 - A_R(c; c) A_{\tilde{x}}(c; c)\}^{-1}$

TABLE A₁. Calculation of the coupled regions ($\{L, \tilde{x}\}, \{R, \tilde{x}\}$) path integral amplitudes in terms of fundamental amplitudes.

Repeating the procedure of the previous paragraph, by substituting the phase event factors and completing the tedious algebra, we find:

$$\Upsilon^{L,\tilde{x},R} = 2 \frac{\text{Im} \tilde{\mathcal{G}}_{r_1}^{\pi/4} \text{Im} \tilde{\mathcal{G}}_{r_2}^{\pi/4}}{\tilde{\mathcal{G}}_b} \left\{ \begin{array}{l} \frac{1}{\text{Re} \tilde{\mathcal{G}}_b - \frac{\tilde{\xi}_b^2 (\pm 2 \text{Im} \tilde{\mathcal{G}}_b \tilde{\xi}_b^{-1} + \text{Re} \tilde{\mathcal{G}}_b)}{4 + \tilde{\xi}_b^2}} + \\ i \frac{\tilde{\xi}_b^2 (\pm 2 \text{Re} \tilde{\mathcal{G}}_b \tilde{\xi}_b^{-1} - \text{Im} \tilde{\mathcal{G}}_b)}{4 + \tilde{\xi}_b^2} \\ - \frac{1}{\text{Re} \tilde{\mathcal{G}}_b - \frac{\tilde{\mathcal{G}}_b \tilde{\xi}_b^2}{4 + \tilde{\xi}_b^2}} \end{array} \right\} \quad (\text{A-4})$$

where the twofold symbols \pm that appear in the first fractional term, mean that we must actually sum two fractions, one for each sign.

iii) Transition Amplitude $\Upsilon^{L,\bar{x},R,\bar{x}}$

In this case state $|0\rangle$ not only interacts with state $|1\rangle$ through the internal barrier but with the field barrier \bar{x} as well. This will force the system to decay. It is obvious that we must first combine the three regions L, \bar{x} , R, by propagating from r_1 to turning point d , and then combine regions \bar{x} , R, \bar{x} , by propagating from d to b , and then alternate the couple (L, \bar{x}) with (R, \bar{x}) in all possible ways. Finally we can propagate to point r_2 through the couple (L, \bar{x}) or by staying entirely at region L. Putting all these together we get:

$$\begin{aligned} \Upsilon^{L,\bar{x},R,\bar{x}} = & \left\{ L \rightleftharpoons_{r_1}^c \bar{x} \right\} A_R(c;d) \left[1 + \left\{ R \rightleftharpoons_c^c \bar{x} \right\} \right] \left[1 - \left\{ R \rightleftharpoons_c^b \bar{x} \right\} \left\{ L \rightleftharpoons_b^c \bar{x} \right\} \right]^{-1} \\ & \left\{ \bar{x} \rightleftharpoons_d^c R \right\} A_{\bar{x}}(c;b) \left[1 + \left\{ \bar{x} \rightleftharpoons_c^c R \right\} \right] \left[1 - \left\{ \bar{x} \rightleftharpoons_c^d R \right\} \left\{ \bar{x} \rightleftharpoons_d^c R \right\} \right]^{-1} \\ & \left[1 - (-i)A_L(r_1;b) \left\{ L \rightleftharpoons_{r_1}^c \bar{x} \right\} A_R(c;d) \left[1 + \left\{ R \rightleftharpoons_c^c \bar{x} \right\} \right] \left[1 - \left\{ R \rightleftharpoons_c^b \bar{x} \right\} \left\{ L \rightleftharpoons_b^c \bar{x} \right\} \right]^{-1} \right]^{-1} \quad (\text{A-5}) \\ & \left[\left\{ \bar{x} \rightleftharpoons_d^c R \right\} A_{\bar{x}}(c;b) \left[1 + \left\{ \bar{x} \rightleftharpoons_c^c R \right\} \right] \left[1 - \left\{ \bar{x} \rightleftharpoons_c^d R \right\} \left\{ \bar{x} \rightleftharpoons_d^c R \right\} \right]^{-1} \right]^{-1} \\ & \left[1 + \left\{ L \rightleftharpoons_b^c \bar{x} \right\} \left\{ R \rightleftharpoons_c^c \bar{x} \right\} \left[1 - \left\{ R \rightleftharpoons_c^b \bar{x} \right\} \left\{ L \rightleftharpoons_b^c \bar{x} \right\} \right]^{-1} \right] \left[1 + \left\{ L \rightleftharpoons_b^c \bar{x} \right\} \right] A_L(b;r_2) \end{aligned}$$

In Table A₂ that follows we have calculated the coupled regions propagation amplitudes of this category, in terms of fundamental amplitudes.

Amplitudes of the regions L, \bar{x} , R	Function of Fundamental Amplitudes
$\left\{ R \rightleftharpoons_c^c \bar{x} \right\}$	$A_R(c;c)A_{\bar{x}}(c;c) \left[1 - A_R(c;c)A_{\bar{x}}(c;c) \right]^{-1}$
$\left\{ L \rightleftharpoons_b^b \bar{x} \right\}$	$A_L(b;b)A_{\bar{x}}(b;b) \left[1 - A_L(b;b)A_{\bar{x}}(b;b) \right]^{-1}$
$\left\{ \bar{x} \rightleftharpoons_c^d R \right\}$	$A_R(c;d)A_{\bar{x}}(c;c) \left[1 - A_R(c;c)A_{\bar{x}}(c;c) \right]^{-1}$
$\left\{ \bar{x} \rightleftharpoons_c^c R \right\}$	$A_R(c;c)A_{\bar{x}}(c;c) \left[1 - A_R(c;c)A_{\bar{x}}(c;c) \right]^{-1}$
$\left\{ \bar{x} \rightleftharpoons_d^c R \right\}$	$A_{\bar{x}}(d;d)A_R(c;d) \left[1 - A_{\bar{x}}(d;d)A_R(c;c) \right]^{-1}$

TABLE A₂. Calculation of the coupled regions ($\{R, \bar{x}\}$, $\{L, \bar{x}\}$, $\{\bar{x}, L\}$) path integral amplitudes in terms of fundamental amplitudes.

The field barrier $\bar{\times}$ acquires a phase factor and forms the following barrier magnitude $\exp\left[-\int_d^e \tau(y)dy\right] \equiv e^{-\gamma(d)} \equiv \bar{\gamma}_d$. Putting the above together and completing the tedious algebra, we finally get:

$$\Upsilon^{L,\bar{\times},R,\bar{\times}} = 2 \frac{\text{Im} \bar{\mathcal{G}}_{r_1}^{\pi/4} \text{Im} \bar{\mathcal{G}}_{r_2}^{\pi/4}}{\bar{\mathcal{G}}_b} \left\{ \begin{array}{l} - \frac{1}{2 \left\{ \text{Re} \bar{\mathcal{G}}_b - \frac{\bar{\xi}_b^2 \left[\begin{array}{l} (\pm 2 \text{Im} \bar{\mathcal{G}}_b \bar{\xi}_b^{-1} + \text{Re} \bar{\mathcal{G}}_b) + \\ i(\pm 2 \text{Re} \bar{\mathcal{G}}_b \bar{\xi}_b^{-1} - \text{Im} \bar{\mathcal{G}}_b) \end{array} \right]}{4 + \bar{\xi}_b^2} \right\}} \\ + \frac{1}{4 \text{Re} \bar{\mathcal{G}}_b - \bar{\xi}_b^2 \bar{\mathcal{G}}_b \pm \frac{\rho}{\bar{\mathcal{G}}_b}} \end{array} \right\} \quad (\text{A-6})$$

where quantity ρ is defined as

$$\rho = \left\{ -4 \bar{\xi}_b^2 \bar{\mathcal{G}}_b^4 + \frac{(4 \bar{\xi}_b \bar{\gamma}_d)^2 \bar{\mathcal{G}}_b^3 \text{Re} \bar{\mathcal{G}}_b}{(4 \text{Re} \bar{\mathcal{G}}_b - \bar{\xi}_b^2 \bar{\mathcal{G}}_b)^2 + (\bar{\xi}_b \bar{\gamma}_d)^2} \right\}^{1/2} \quad (\text{A-7})$$

Again the symbol \pm that appears in eq. (18), means that we must actually sum two fractions, one for each sign.

iv) Transition Amplitude $\Upsilon^{L,\bar{\times},R,\bar{\times},\bar{\times}}$

State $|1\rangle$ has already interacted with the total region on its right side, before reaching point a in order to interact with the second field barrier $\bar{\times}$. A second channel of decay appears now. Thus we need to modify all the previously calculated transition amplitudes in such a way that propagation ends at turning point a instead of r_2 . Thus we use the symbol $\Upsilon^{L+\bar{\times}+R+\bar{\times}}(r_1;a)$ to describe the sum of the previously calculated amplitudes for $r_2 = a$. Modifying in this way the amplitudes we get:

$$\Upsilon_{r_1 \rightarrow a}^L = \bar{A}_L(r_1;a) + \bar{A}_L(r_1;a)(-i)A_L(a;a) + \bar{A}_L(r_1;b)(-i)A_L(b;a) \quad (\text{A-8})$$

$$\Upsilon_{r_1 \rightarrow a}^{L,\bar{\times}} = A_L(r_1;b)A_{\bar{\times}}(b;b) \{1 - A_L(b;b)A_{\bar{\times}}(b;b)\}^{-1} A_L(b;a) \quad (\text{A-9})$$

$$\Upsilon_{r_1 \rightarrow a}^{L,\bar{\times},R} = \{L \leftrightarrow_{r_1}^c \bar{\times}\} \{R \leftrightarrow_c^b \bar{\times}\} [1 - \{L \leftrightarrow_b^c \bar{\times}\} \{R \leftrightarrow_c^b \bar{\times}\}]^{-1} [\{L \leftrightarrow_b^c \bar{\times}\} A_L(b;a)] \quad (\text{A-10})$$

$$\begin{aligned}
\Upsilon_{r_1 \rightarrow a}^{L, \bar{x}, R, \bar{x}} &= \left\{ L \rightleftharpoons_{r_1}^c \bar{x} \right\} A_R(c; d) \left[1 + \left\{ R \rightleftharpoons_c^c \bar{x} \right\} \right] \left[1 - \left\{ R \rightleftharpoons_b^b \bar{x} \right\} \left\{ R \rightleftharpoons_b^c \bar{x} \right\} \right]^{-1} \\
&\quad \left\{ \bar{x} \rightleftharpoons_d^c R \right\} A_{\bar{x}}(c; b) \left[1 + \left\{ \bar{x} \rightleftharpoons_c^c R \right\} \right] \left[1 - \left\{ \bar{x} \rightleftharpoons_d^d R \right\} \left\{ \bar{x} \rightleftharpoons_d^c R \right\} \right]^{-1} \\
&\quad \left[1 - (-i) A_L(r_1; b) \left\{ L \rightleftharpoons_{r_1}^c \bar{x} \right\} A_R(c; d) \left[1 + \left\{ R \rightleftharpoons_c^c \bar{x} \right\} \right] \left[1 - \left\{ R \rightleftharpoons_b^b \bar{x} \right\} \left\{ L \rightleftharpoons_b^c \bar{x} \right\} \right]^{-1} \right]^{-1} \\
&\quad \left[\left\{ \bar{x} \rightleftharpoons_v^d R \right\} A_{\bar{x}}(c; b) \left[1 + \left\{ \bar{x} \rightleftharpoons_c^c R \right\} \right] \left[1 - \left\{ \bar{x} \rightleftharpoons_d^d R \right\} \left\{ \bar{x} \rightleftharpoons_d^c R \right\} \right]^{-1} \right]^{-1} \\
&\quad \left[1 + \left\{ L \rightleftharpoons_b^c \bar{x} \right\} \left\{ R \rightleftharpoons_c^c \bar{x} \right\} \left[1 - \left\{ R \rightleftharpoons_b^b \bar{x} \right\} \left\{ L \rightleftharpoons_b^c \bar{x} \right\} \right]^{-1} \right] \left[1 + \left\{ L \rightleftharpoons_b^b \bar{x} \right\} \right] A_L(b; a)
\end{aligned} \tag{A-11}$$

Obviously

$$\Upsilon_{r_1 \rightarrow a}^{L+\bar{x}+R+\bar{x}}(r_1; a) = \Upsilon_{r_1 \rightarrow a}^L + \Upsilon_{r_1 \rightarrow a}^{L, \bar{x}} + \Upsilon_{r_1 \rightarrow a}^{L, \bar{x}, R} + \Upsilon_{r_1 \rightarrow a}^{L, \bar{x}, R, \bar{x}} \tag{A-12}$$

The combination of the above with the field barrier \bar{x} , according to our aforementioned directions, gives the following:

$$\begin{aligned}
\Upsilon^{L, \bar{x}, R, \bar{x}, \bar{x}} &= \left[\Upsilon^{L+\bar{x}+R+\bar{x}}(r_1; a) A_{\bar{x}}(a; a) + \left(\Upsilon^{L+\bar{x}+R+\bar{x}}(r_1; a) A_{\bar{x}}(a; a) \right)^2 + \dots \right] A_L(a; a) = \\
&\quad \Upsilon^{L+\bar{x}+R+\bar{x}}(r_1; a) A_{\bar{x}}(a; a) \left[1 - \Upsilon^{L+\bar{x}+R+\bar{x}}(r_1; a) A_{\bar{x}}(a; a) \right]^{-1} A_L(a; a)
\end{aligned} \tag{A-13}$$

where a single propagation inside field barrier \bar{x} acquires a phase factor that forms the following barrier magnitude $\exp \left[- \left| \int_0^a \tau(y) dy \right| \right] \equiv e^{-\delta(a)} \equiv \widehat{\delta}_a$ and where of course

$$A_{\bar{x}}(a; a) = \frac{i}{2} \frac{\widehat{\delta}_a^2}{1 + \widehat{\delta}_a^2 / 4}$$

Putting all these together we get the total transition amplitude for propagation between points r_1 and a in the following form

$$\begin{aligned}
\Upsilon^{total} &= \Upsilon^{L+\bar{x}+R+\bar{x}}(r_1; a) + \Upsilon^{L, \bar{x}, R, \bar{x}, \bar{x}} \Rightarrow \\
\Upsilon^{total} &= \Upsilon^{L+\bar{x}+R+\bar{x}}(r_1; a) + \frac{\Upsilon^{L+\bar{x}+R+\bar{x}}(r_1; a) A_{\bar{x}}(\alpha; \alpha) A_L(\alpha; \alpha)}{1 - \Upsilon^{(0)+\bar{x}+1)+\bar{x}}(r_1; a) A_{\bar{x}}(a; a)} \Rightarrow \\
\Upsilon^{total} &= \frac{\Upsilon^{L+\bar{x}+R+\bar{x}}(r_1; a) A_{\bar{x}}(\alpha; \alpha) \left\{ \left(\frac{1}{2 \widehat{\delta}_b \operatorname{Re} \widehat{\delta}_b} \right) - \Upsilon^{L+\bar{x}+R+\bar{x}}(r_1; a) \right\} + \Upsilon^{L+\bar{x}+R+\bar{x}}(r_1; a)}{1 - \Upsilon^{L+\bar{x}+R+\bar{x}}(r_1; a) A_{\bar{x}}(a; a)}
\end{aligned} \tag{A-14}$$

It is interesting to notice that the pole condition: $1 - \Upsilon^{L+\bar{x}+R+\bar{x}}(r_1; a) A_{\bar{x}}(a; a) = 0$, transforms the total amplitude in its much simpler form

$$\Upsilon^{total} = \frac{1}{2 \left\{ 1 - \Upsilon^{L+\tilde{x}+R+\tilde{x}}(r_1; a) A_{\tilde{x}}(a; a) \right\} \tilde{\mathcal{G}}_b \operatorname{Re} \tilde{\mathcal{G}}_b} \quad (\text{A-15})$$

APPENDIX B:

Analytic calculation of the energy poles of each propagation amplitude beyond that of region L.

Regions L and \tilde{x} contribute with the extra pole term:

$$Pole^{L, \tilde{x}} \sim \left\{ \operatorname{Re} \tilde{\mathcal{G}}_b - \frac{\tilde{\xi}_b^2 \tilde{\mathcal{G}}_b}{4 + \tilde{\xi}_b^2} \right\}^{-1} \quad (\text{B-1})$$

It is obvious however, that the complex denominator of the above fraction cannot be in any way equal to zero. Thus, we expand the denominator around the eigenvalues of the isolated unperturbed well. Doing so we find

$$Pole_n^{L, \tilde{x}} \sim \left\{ E - \left\{ E_n - \tilde{\xi}_{b,n}^2 \frac{d\tilde{\xi}(b)}{dE_n} \left(2\sqrt{2} \frac{d\tilde{\mathcal{G}}(b)}{dE_n} \right)^{-2} - i \left(\frac{d\tilde{\mathcal{G}}(b)}{dE_n} \right)^{-1} \frac{\tilde{\xi}_{b,n}^2}{4} \right\} \right\}^{-1} \quad (\text{B-2})$$

Thus the perturbed eigenvalues become complex and equal to

$$Z_n^{L, \tilde{x}} = E_n - \tilde{\xi}_{b,n}^2 \left\{ d^{E_n} \tilde{\xi}(b) \right\} \left(2\sqrt{2} \left\{ d^{E_n} \tilde{\mathcal{G}}(b) \right\} \right)^{-2} - i \left(d^{E_n} \tilde{\mathcal{G}}(b) \right)^{-1} \frac{\tilde{\xi}_{b,n}^2}{4} \quad (\text{B-3})$$

where the subscript n denotes calculation on the eigenvalue E_n and where the symbol d^{E_n} denotes derivation with respect to the eigenvalue E_n .

- i) Regions L, \tilde{x} and R contribute with two extra pole terms (one for each sign):

$$Pole^{L, \tilde{x}, R} \sim \left\{ 2 \left\{ \operatorname{Re} \tilde{\mathcal{G}}_b - \frac{\tilde{\xi}_b^2 \left(\pm 2 \operatorname{Im} \tilde{\mathcal{G}}_b \tilde{\xi}_b^{-1} + \operatorname{Re} \tilde{\mathcal{G}}_b \right)}{4 + \tilde{\xi}_b^2} + i \frac{\tilde{\xi}_b^2 \left(\pm 2 \operatorname{Re} \tilde{\mathcal{G}}_b \tilde{\xi}_b^{-1} - \operatorname{Im} \tilde{\mathcal{G}}_b \right)}{4 + \tilde{\xi}_b^2} \right\} \right\}^{-1} \quad (\text{B-4})$$

The two fold signs that appear in the above formula translate to the doublet splitting that was previously described. Hence, we develop the denominator of the above fraction around the eigenvalues E_n of the unperturbed well, to get

$$Pole_n^{L,\bar{x},R} \sim \frac{1}{E - E_n + \frac{\widehat{\xi}_{b,n}(\mp 2 - i\widehat{\xi}_{b,n})}{\left\{ \left\{ d^{E_n} \bar{g}(b) \right\} \left(-4 + \widehat{\xi}_{b,n}^2 \right) \pm 2 \left\{ d^{E_n} \widehat{\xi}(b) \right\} \widehat{\xi}_{b,n}^2 + i 2 \widehat{\xi}_{b,n} \left\{ \left\{ d^{E_n} \widehat{\xi}(b) \right\} \widehat{\xi}_{b,n} \mp \left\{ d^{E_n} \bar{g}(b) \right\} \right\} \right}}$$
(B-5)

The perturbed eigenvalues become then complex and equal to

$$Z_n^{L,\bar{x},R} = E_n - \frac{\left\{ \mp \frac{\widehat{\xi}_{b,n}}{2} \left\{ -\left\{ d^{E_n} \bar{g}(b) \right\} \left(1 - \frac{\widehat{\xi}_{b,n}^2}{4} \right) \pm \left\{ d^{E_n} \widehat{\xi}(b) \right\} \frac{\widehat{\xi}_{b,n}}{2} \right\} \right.}{\left. \left\{ -i \frac{\widehat{\xi}_{b,n}}{2} \left\{ -\left\{ d^{E_n} \bar{g}(b) \right\} \frac{\widehat{\xi}_{b,n}}{2} \left(1 - \frac{\widehat{\xi}_{b,n}^2}{4} \right) \pm \left\{ d^{E_n} \widehat{\xi}(b) \right\} \frac{\widehat{\xi}_{b,n}^2}{4} + \left\{ d^{E_n} \widehat{\xi}(b) \right\} \widehat{\xi}_{b,n}^2 \mp \left(\left\{ d^{E_n} \bar{g}(b) \right\} \right) \right\} \right\}}{\left\{ -\left\{ d^{E_n} \bar{g}(b) \right\} \left(1 - \frac{\widehat{\xi}_{b,n}^2}{4} \right) \pm \left\{ d^{E_n} \widehat{\xi}(b) \right\} \frac{\widehat{\xi}_{b,n}}{2} \right\}^2 + \frac{\widehat{\xi}_{b,n}}{2} \left\{ \left\{ d^{E_n} \widehat{\xi}(b) \right\} \widehat{\xi}_{b,n} \mp \left(\left\{ d^{E_n} \bar{g}(b) \right\} \right) \right\}^2}$$
(B-6)

- ii) Regions L, \bar{x}, R, \bar{x} contribute with two extra pole terms (one for each sign), coming through the fraction:

$$Pole^{L,\bar{x},R,\bar{x}} \sim \frac{1}{4 \operatorname{Re} \bar{g}_b - \widehat{\xi}_b^2 \bar{g}_b \pm \bar{g}_b^{-1} \rho} \Rightarrow$$

$$Pole^{L,\bar{x},R,\bar{x}} \sim \frac{1}{4 \operatorname{Re} \bar{g}_b - \widehat{\xi}_b^2 \bar{g}_b \pm \left\{ -4 \widehat{\xi}_b^2 \bar{g}_b^2 + \frac{\left(4 \widehat{\xi}_b \widehat{\gamma}_d \right)^2 \bar{g}_b \operatorname{Re} \bar{g}_b}{\left(4 \operatorname{Re} \bar{g}_b - \widehat{\xi}_b^2 \bar{g}_b \right)^2 + \left(\widehat{\xi}_b \widehat{\gamma}_d \right)^2} \right\}^{1/2}}$$
(B-7)

For once more, we develop the denominator around the eigenvalues E_n of the unperturbed well to get

$$Pole_n^{L,\bar{x},R,\bar{x}} \sim \left\{ (E - E_n) \left\{ \begin{array}{l} \left(-i \widehat{\xi}_{b,n} \mp 2 \right) + \\ \left[-4 \left\{ d^{E_n} \bar{g}(b) \right\} + 2i \widehat{\xi}_{b,n}^2 \left\{ d^{E_n} \widehat{\xi}(b) \right\} + \left\{ d^{E_n} \bar{g}(b) \right\} \widehat{\xi}_{b,n}^2 \right. \\ \left. \mp \widehat{\xi}_{b,n} \left(-2 \left\{ d^{E_n} \widehat{\xi}(b) \right\} + 2i \left\{ d^{E_n} \bar{g}(b) \right\} - 4i \frac{\left\{ d^{E_n} \bar{g}(b) \right\} e^{-2\gamma_n(\nu)}}{\widehat{\gamma}_{d,n}^2 - \widehat{\xi}_{b,n}^2} \right) \right] \end{array} \right\} \right\}^{-1}$$
(B-8)

Thus the perturbed eigenvalues become complex and equal to

$$\begin{aligned}
 Z_n^{L, \tilde{\times}, R, \tilde{\times}} = E_n - & \frac{\left\{ \mp 2 \tilde{\xi}_{b,n} \left\{ \{d^{E_n} \tilde{\mathcal{G}}(b)\} (4 - \tilde{\xi}_{b,n}^2) \pm 2 \tilde{\xi}_{b,n}^2 \{d^{E_n} \tilde{\xi}(b)\} \right\} + 2 \tilde{\xi}_{b,n}^4 \left\{ \{d^{E_n} \tilde{\xi}(b)\} \mp \tilde{\xi}_{b,n} \{d^{E_n} \tilde{\mathcal{G}}(b)\} - 2 \frac{\{d^{E_n} \tilde{\mathcal{G}}(b)\} \tilde{\gamma}_{d,n}^2}{(\tilde{\gamma}_{d,n} \tilde{\xi}_{b,n})^2 - \tilde{\xi}_{b,n}^4} \right\} \right\}}{\left\{ \{d^{E_n} \tilde{\mathcal{G}}(b)\} (4 - \tilde{\xi}_{b,n}^2) \pm 2 \tilde{\xi}_{b,n}^2 \{d^{E_n} \tilde{\xi}(b)\} \right\}^2 + \left\{ 2 \tilde{\xi}_{b,n}^2 \left\{ \{d^{E_n} \tilde{\xi}(b)\} \mp \tilde{\xi}_{b,n}^{-1} \{d^{E_n} \tilde{\mathcal{G}}(b)\} - 2 \frac{\{d^{E_n} \tilde{\mathcal{G}}(b)\} \tilde{\gamma}_{d,n}^2}{(\tilde{\gamma}_{d,n} \tilde{\xi}_{b,n})^2 - \tilde{\xi}_{b,n}^4} \right\} \right\}^2} \\
 + i & \frac{\left\{ \mp 4 \tilde{\xi}_{b,n}^3 \left(\frac{1}{2} \{d^{E_n} \tilde{\xi}(b)\} \mp \frac{\tilde{\xi}_{b,n}}{4} \{d^{E_n} \tilde{\mathcal{G}}(b)\} \pm \{d^{E_n} \tilde{\mathcal{G}}(b)\} \frac{\tilde{\gamma}_{d,n}^2 \tilde{\xi}_{b,n}^{-1}}{\tilde{\gamma}_{d,n}^2 - \tilde{\xi}_{b,n}^2} \right) \right\}}{\left\{ \{d^{E_n} \tilde{\mathcal{G}}(b)\} (4 - \tilde{\xi}_{b,n}^2) \pm 2 \tilde{\xi}_{b,n}^2 \{d^{E_n} \tilde{\xi}(b)\} \right\}^2 + \left\{ 2 \tilde{\xi}_{b,n}^2 \left\{ \{d^{E_n} \tilde{\xi}(b)\} \mp \tilde{\xi}_{b,n}^{-1} \{d^{E_n} \tilde{\mathcal{G}}(b)\} - 2 \frac{\{d^{E_n} \tilde{\mathcal{G}}(b)\} \tilde{\gamma}_{d,n}^2}{(\tilde{\gamma}_{d,n} \tilde{\xi}_{b,n})^2 - \tilde{\xi}_{b,n}^4} \right\} \right\}^2}
 \end{aligned} \tag{B-9}$$

- iii) Regions $L, \tilde{\times}, R, \tilde{\times}$ and $\tilde{\times}$ contribute with two extra pole terms, (one for each sign), arising through the following condition as this is induced by eq. (23):

$$\begin{aligned}
 4 \operatorname{Re} \tilde{\mathcal{G}}_b - \tilde{\xi}_b^2 \tilde{\mathcal{G}}_b \pm & \left(-4 \left(\tilde{\xi}_b \tilde{\mathcal{G}}_b \right)^2 + \frac{\left(4 \tilde{\xi}_b \tilde{\gamma}_d \right)^2 \tilde{\mathcal{G}}_b \operatorname{Re} \tilde{\mathcal{G}}_b(\lambda)}{\left(4 \operatorname{Re} \tilde{\mathcal{G}}_b - \tilde{\xi}_b^2 \tilde{\mathcal{G}}_b \right)^2 + \left(\tilde{\xi}_b \tilde{\gamma}_d \right)^2} \right)^{1/2} \\
 - (1+i) \{ \operatorname{Re} \tilde{\mathcal{G}}_b + \operatorname{Im} \tilde{\mathcal{G}}_b \} & \frac{1}{1 + 4 \tilde{\delta}_a^{-2}} = 0
 \end{aligned} \tag{B-10}$$

We develop the above quantity around the eigenvalues E_n of the unperturbed wells and impose the:

$$\begin{aligned}
 & -i \left(\tilde{\xi}_{b,n}^2 + \frac{\tilde{\delta}_{a,n}^2}{4} \right) \mp 2 \tilde{\xi}_{b,n} - \frac{\tilde{\delta}_{a,n}^2}{4} + \\
 (E - E_n) & \left\{ \begin{aligned}
 & \left\{ \{d^{E_n} \tilde{\mathcal{G}}(b)\} \left(-4 + \tilde{\xi}_{b,n}^2 - \frac{\tilde{\delta}_{a,n}^2}{4} \right) + 2i \tilde{\xi}_{b,n}^2 \{d^{E_n} \tilde{\xi}(b)\} - \{d^{E_n} \tilde{\delta}(a)\} \frac{\tilde{\delta}_{a,n}^2}{2} \right\} \\
 & \mp \tilde{\xi}_{b,n} \left(-2 \{d^{E_n} \tilde{\xi}(b)\} + 2i \{d^{E_n} \tilde{\mathcal{G}}(b)\} - 4i \{d^{E_n} \tilde{\mathcal{G}}(b)\} \frac{\tilde{\gamma}_{d,n}^2}{\tilde{\gamma}_{d,n}^2 - \tilde{\xi}_{b,n}^2} \right) \\
 & -i \left(\frac{1}{2} \{d^{E_n} \tilde{\mathcal{G}}(b)\} + \{d^{E_n} \tilde{\delta}(a)\} \right) \frac{\tilde{\delta}_{a,n}^2}{2}
 \end{aligned} \right\} = 0
 \end{aligned} \tag{B-11}$$

Thus, once more the perturbed eigenvalues become complex and equal to

$$\begin{aligned}
Z_n^{L,\tilde{x},R,\tilde{x},\tilde{x}} = E_n - & \left\{ \left(\mp 2\tilde{\xi}_{b,n} - \frac{\tilde{\delta}_{a,n}^2}{4} \right) \left\{ d^{E_s} \tilde{g}(b) \left(4 + \tilde{\xi}_{b,n}^2 - \frac{\tilde{\delta}_{a,n}^2}{4} \right) - \frac{\tilde{\delta}_{a,n}^2}{2} \{ d^{E_s} \tilde{\delta}(a) \} \pm 2\tilde{\xi}_{b,n} \{ d^{E_s} \tilde{\xi}(b) \} \right\} \right. \\
& \left. + \left(-2\tilde{\xi}_{b,n}^2 - \frac{\tilde{\delta}_{a,n}^2}{4} \right) \left\{ 2\tilde{\xi}_{b,n}^2 \left(\{ d^{E_s} \tilde{\xi}(b) \} \mp \tilde{\xi}_{b,n}^{-1} \{ d^{E_s} \tilde{g}(b) \} \pm 2 \{ d^{E_s} \tilde{g}(b) \} \frac{\tilde{\xi}_{b,n}^{-1} \tilde{\gamma}_{d,n}^2}{\tilde{\gamma}_{d,n}^2 - \tilde{\xi}_{b,n}^2} \right) - \frac{\tilde{\delta}_{a,n}^2}{2} \left(\frac{1}{2} \{ d^{E_s} \tilde{g}(b) \} + \{ d^{E_s} \tilde{\delta}(a) \} \right) \right\} \right\} \\
& \left\{ \left\{ d^{E_s} \tilde{g}(b) \left(-4 + \tilde{\xi}_{b,n}^2 - \frac{\tilde{\delta}_{a,n}^2}{4} \right) \pm 2\tilde{\xi}_{b,n} \{ d^{E_s} \tilde{\xi}(b) \} - \frac{\tilde{\delta}_{a,n}^2}{2} \{ d^{E_s} \tilde{\delta}(a) \} \right\}^2 + \right. \\
& \left. \left\{ 2\tilde{\xi}_{b,n}^2 \left(\{ d^{E_s} \tilde{\xi}(b) \} \mp \tilde{\xi}_{b,n}^{-1} \{ d^{E_s} \tilde{g}(b) \} \pm 2 \{ d^{E_s} \tilde{g}(b) \} \frac{\tilde{\xi}_{b,n}^{-1} \tilde{\gamma}_{d,n}^2}{\tilde{\gamma}_{d,n}^2 - \tilde{\xi}_{b,n}^2} \right) - \frac{\tilde{\delta}_{a,n}^2}{2} \left(\frac{1}{2} \{ d^{E_s} \tilde{g}(b) \} + \{ d^{E_s} \tilde{\delta}(a) \} \right) \right\}^2 \right\} \\
+ i & \left\{ \left(\mp 2e^{-\theta(\tilde{\lambda}_s)} - \frac{e^{-2\theta_s(\tilde{\lambda}_s)}}{4} \right) \left\{ 2e^{-2\theta_s(\tilde{\lambda}_s)} \left(\{ d^{E_s} \tilde{\xi}(b) \} \mp e^{\theta_s(\tilde{\lambda}_s)} \{ d^{E_s} \tilde{g}(b) \} \pm 2 \{ d^{E_s} \tilde{g}(b) \} \frac{e^{-2\theta_s(\tilde{\lambda}_s)}}{e^{-2\theta_s(\tilde{\lambda}_s)} - e^{-2\theta_s(\tilde{\lambda}_s)}} \right) - \frac{\tilde{\delta}_{a,n}^2}{2} \left(\frac{1}{2} \{ d^{E_s} \tilde{g}(b) \} + \{ d^{E_s} \tilde{\delta}(a) \} \right) \right\} + \right. \\
& \left. \left(e^{-\theta(\tilde{\lambda}_s)} + \frac{\tilde{\delta}_{a,n}^2}{4} \right) \left\{ \{ d^{E_s} \tilde{g}(b) \} \left(-4 + \tilde{\xi}_{b,n}^2 - \frac{\tilde{\delta}_{a,n}^2}{4} \right) \pm 2e^{-\theta_s(\tilde{\lambda}_s)} \{ d^{E_s} \tilde{\xi}(b) \} - \frac{\tilde{\delta}_{a,n}^2}{2} \{ d^{E_s} \tilde{\delta}(a) \} \right\} \right\} \\
& \left\{ \left\{ d^{E_s} \tilde{g}(b) \left(-4 + \tilde{\xi}_{b,n}^2 - \frac{\tilde{\delta}_{a,n}^2}{4} \right) \pm 2\tilde{\xi}_{b,n} \{ d^{E_s} \tilde{\xi}(b) \} - \frac{\tilde{\delta}_{a,n}^2}{2} \{ d^{E_s} \tilde{\delta}(a) \} \right\}^2 + \right. \\
& \left. \left\{ 2\tilde{\xi}_{b,n}^2 \left(\{ d^{E_s} \tilde{\xi}(b) \} \mp \tilde{\xi}_{b,n}^{-1} \{ d^{E_s} \tilde{g}(b) \} \pm 2 \{ d^{E_s} \tilde{g}(b) \} \frac{\tilde{\xi}_{b,n}^{-1} \tilde{\gamma}_{d,n}^2}{\tilde{\gamma}_{d,n}^2 - \tilde{\xi}_{b,n}^2} \right) - \frac{\tilde{\delta}_{a,n}^2}{2} \left(\frac{1}{2} \{ d^{E_s} \tilde{g}(b) \} + \{ d^{E_s} \tilde{\delta}(a) \} \right) \right\}^2 \right\}
\end{aligned}
\tag{B-12}$$

REFERENCES

- [1] N. S. Yanofsky and M.A. Mannucci, Quantum Computing, Cambridge: Cambridge University Press, 2008, pp. 138-142.
- [2] T. Hey, Comput. Control Eng. J., 10(3), 105, (1999).
- [3] E. Rieffel and W. Polak, ACM Comput. Surv., 32(3), 300, (2000).
- [4] M. Russ and G. Burkard, J. Phys. Condensed Matter, 29(39), 393001, (2017).
- [5] X.-Y. Zhu, T. Tu, A.-L. Guo, Z.-Q. Zhou, C.-F. Li, and G.-C. Guo, Sci. Rep., 8(1), 15761, (2018).
- [6] T. Fujisawa, T. Hayashi, H. D. Cheong, Y. H. Jeong, and Y. Hirayama, Phys. E, Low-Dimensional Syst. Nanostruct., 21(2) 1052, (2004).
- [7] A. Weichselbaum and S. Ulloa, Phys. Rev. A, Gen. Phys., 70(3), 032328, (2004).
- [8] D. P. K. Bladh and T. Duty, New J. Phys., 7(1), 180, (2005).
- [9] M. Lutchyn, .. Cywiski, C. P. Nave, and S. Das Sarma, Phys. Rev. B, Condens. Matter, 78(2), 024508, (2008).
- [10] M. Gonzalez-Zalba. (2018). "Solid state qubits." [Online]. Available: <https://arxiv.org/abs/1801.06722>
- [11] T. Stievater *et al.*, Phys. Rev. Lett., 87(13), 133603, (2001).
- [12] S. Datta, Quantum Transport: Atom to Transistor. Cambridge, U.K.: Cambridge Univ. Press, 2005, pp. 47-52.
- [13] C.H. Townes, and A.L. Schawlow, Microwave Spectroscopy, New York: Dover Publications, 1975, pp. 300-307.
- [14] R.P. Feynman, R.B. Leighton, and M. Sands, The Feynman Lectures on Physics, Volume III, Massachusset: Addison-Wesley, Reading, 1963, pp. 115-129.

- [15] G.J. Milburn, J. Corney, E.M. Wright and D.F. Walls, *Physical Review A*, 55(6), 4318, (1997).
- [16] Y. Shin, M. Saba, T.A. Pasquini, W. Ketterle, D.E. Pritchard and A.E. Leanhardt, *Phys. Rev. Lett.*, 92(5), 050405, (2004).
- [17] D. Dast, D. Haag, H. Cartarius, G. Wunner, R. Eichler and J. Main, *Fortschritte der Physik*, 61(2-3), 124-139, (2013).
- [18] J.L. Baudour, H.T. Cailleau and W.B. Yelon, *Acta Crystallographica Section B: Structural Crystallography and Crystal Chemistry*, 33(6), 1773-1780, (1977).
- [19] T. Schumm, S. Hofferberth, L.M. Andersson, S. Wildermuth, S. Groth, I. Bar-Joseph, ... and P. Krüger, *Nature Physics*, 1(1), 57-62, (2005).
- [20] A. Landau, Y. Aharonov and E. Cohen, *International Journal of Quantum Information*, 14(05), 1650029, (2016).
- [21] L. Pezzé, A. Smerzi, G.P. Berman, A.R. Bishop and L.A. Collins, *Physical Review A*, 74(3), 033610, (2006).
- [22] I. L. Chuang and Y. Yamamoto, *Phys. Rev. A* 52, 3489, (1995); *Phys. Rev. Lett.* 76, 4281 (1996).
- [23] Y. Aharonov, E. Cohen, A. Landau and A. Elitzur, *Scientific reports*, 7(1), 1-9, (2017)
- [24] M. Lodari, A. Tosato, D. Sabbagh, M.A. Schubert, G. Capellini, A. Sammak, A., ... & G. Scappucci, G., *Physical Review B*, 100(4), 041304, (2019).
- [25] C. Adami and N. J. Cerf, *Quantum computation with linear optics*. In *NASA International Conference on Quantum Computing and Quantum Communications* (pp. 391-401). Springer, Berlin, Heidelberg, (1998).
- [26] X.Q. Li, and Y. Arakawa, Y. (2000). *Phys. Rev. A*, 63(1), 012302, (2000).
- [27] J. Gorman, D.G. Hasko, and D.A. Williams, *Phys. Rev. Lett.* 95(9), 090502, (2005).
- [28] P. Giounanlis, E. Blokhina, K. Pomorski, D.R. Leipold, and R.B. Staszewski, *IEEE Access*, 7, 49262, 92019).
- [29] T.P. Orlando, S. Lloyd, L.S. Levitov, K.K. Berggren, M.J. Feldman, M.F., Bocko, and C.H. Van der Wal, *Physica C: Superconductivity*, 372,194, (2002).
- [30] R.H. Koch, G.A. Keefe, F.P. Milliken, J.R. Rozen, C.C. Tsuei, J.R. Kirtley, and D.P. DiVincenzo, *Phys. Rev. Lett.* 96(12), 127001, (2006).
- [31] M.G. Castellano, F. Chiarello, P. Carelli, C. Cosmelli, F. Mattioli and G. Torrioli *New Journal of Physics*, 12(4), 043047, (2010).
- [32] R. Malek, and K.P. Wanczek, *Rapid communications in mass spectrometry*, 11(14), 1616-1618, (1997).
- [33] A. Retzker, R.C. Thompson, D.M. Segal, and M.B. Plenio *Phys. Rev. Lett.* 101(26), 260504, (2008).
- [34] N. Friis, O. Marty, C. Maier, C. Hempel, M. Holzäpfel, P. Jurcevic and B. Lanyon, *Physical Review X*, 8(2), 021012, (2018).
- [35] C.J. Foot and M.D. Shotton, *Am. J. Phys.*, 79(7), 762(2011).
- [36] W. Dür and S. Heusler, "What we can learn about quantum physics from a single qubit." *arXiv preprint arXiv:1312.1463* (2013).
- [37] A. Landau, Y. Aharonov, and E. Cohen, *Int. J. Quant. Inf.*, 14(05), 1650029(2016).
- [38] M.D. Kim, D. Shin, and J. Hong, *J. Phys. Rev. B*, 68(13), 134513, (2003).
- [39] Y. V. Fominov, A.A. Golubov, and M.Y. Kupriyanov, *Journal of Experimental and Theoretical Phys. Lett*, 77(10), 587, (2003).
- [40] P.D. Shaju, , V. C. Kuriakose *Physica C*, 424(3), 125(2005).
- [41] R.J. Monaco, *Phys. C*, 28(44), 445702, (2016).
- [42] S. Savel'ev, X. Hu and F. Nori, *New J. Phys.*, 8(6), 105, (2006).

- [43] K.M. Indlekofer, T. Schäpers, T. On the Possibility of Using Semiconductor Nanocolumns for the Realization of Quantum Bits. arXiv preprint cond-mat/0703520, (2007).
- [44] V. Ivády, J. Davidsson, N. Deegan, A.L. Falk, P. V. Klimov, S.J. Whiteley, and A. Gali, *Nature communications*, 10(1), 1-8, (2019).
- [45] J.C. Abadillo-Uriel, M.J. Calderón, *New J. Phys.*, 19(4), 043027, (2017).
- [46] P. Jakubczyk, K. Majchrowski, I. Tralle, *Acta Physica Polonica A*, 132(1), 115(2017).
- [47] N.W. Hendrickx, D.P. Franke, A. Sammak, G. Scappucci and M. Veldhorst, *Nature*, 577(7791), 487, (2020).
- [48] D. Loss and D. P. DiVincenzo. *Phys. Rev. A*, 57(1), 120, (1998).
- [49] J.A. Schreier, A. A. Houck, J. Koch, D.I. Schuster, B.R. Johnson, J.M. Chow, ... and R.J. Schoelkopf, *Phys. Rev. B*, 77(18), 180502, (2008).
- [50] T.G. Douvropoulos and C.A. Nicolaides, *J. Chem. Phys.*, 119, 8235, (2003).
- [51] T.G. Douvropoulos and C.A. Nicolaides, *I. J. Quant. Chem.*, 106, 1032, (2006).
- [52] E. Merzbacher, *Quantum Mechanics*, New York: John Wiley, 1998, pp.320-326.
- [53] R.P. Feynman and A.R. Hibbs, *Quantum Mechanics and Path Integrals*, New York: McGraw-Hill, 1965, pp. 31-39.
- [54] M. Razavy, *Quantum Theory of Tunneling*, New Jersey: World Scientific, 2003, pp. 219-220.
- [55] M.C. Gutzwiller, *J. Math. Phys.*, 12, 343, (1971).
- [56] W.H. Miller, *J. Chem. Phys.*, 56, 38, (1972).
- [57] W.H. Miller and T.F. George, *J. Chem. Phys.* 56, 5668, (1972).
- [58] B.R. Holstein and A.R. Swift, *Am. J. Phys.* 50, 829, (1982).
- [59] H. Kleinert, *Path Integrals*, New Jersey: World Scientific, 1995, pp. 199-226.
- [60] L.D. Landau and E.M. Lifshitz, *Quantum Mechanics*, 2nd ed., Oxford: Pergamon Press, 1965, pp. 183-184.
- [61] C.C. Gerry and P.L. Knight, *Introductory Quantum Optics*, Cambridge: Cambridge University Press, 2005, pp. 90-93.
- [62] S. Flugge, *Practical Quantum Mechanics*, Berlin Heidelberg: Springer-Verlag, 1999, pp. 365-368.
- [63] T.G. Douvropoulos and C.A. Nicolaides, *Phys. Rev. A*, 69, 032105, (2004).
- [64] C.J. Myatt, B.E. King, Q.A. Turchette, C.A. Sackett, D. Kielpinski, W.M. Itano, ... & D.J. Wineland, *Nature*, 403(6767), 269, (2000).
- [65] S. Sarkar, S. Paul, C. Vishwakarma, S. Kumar, G.Verma, M. Sainath, ... & M.S. Santhanam, *Phys. Rev. Lett.* 118(17), 174101, (2017).
- [66] L.F. Qiao, A. Streltsov, J. Gao, S. Rana, R.J. Ren, Z.Q. Jiao, ... & X.M. Jin *Phys. Rev. A*, 98(5), 052351, (2018).

Approximate solutions of Maxwell's equations for a charging capacitor

C. J. Papachristou

Department of Physical Sciences, Hellenic Naval Academy
papachristou@hna.gr

Abstract. In previous articles we derived a system of partial differential equations by means of which one may obtain expressions for the electromagnetic field in the interior and the exterior of a charging capacitor. In the present article a recursive process is described for finding solutions of this system in power-series form with respect to time. This allows one to find approximate solutions of Maxwell's equations in a number of situations of physical interest.

Keywords: Maxwell's equations, Faraday's law, charging capacitor

1. Introduction

In previous articles [1,2] we described a mathematical process for finding expressions for the electromagnetic (e/m) field – i.e., solutions of Maxwell's equations – in the interior and the exterior of a charging capacitor. These solutions generalize the “classical” results found in the educational literature of electrodynamics [3-9], which results were noted to not satisfy, in general, the Faraday-Henry law (Maxwell's third equation).

Our method was based on a simple idea: we started with the known (incomplete) solutions and “corrected” them by adding unknown functions to be determined by using the Maxwell system. This led to a system of partial differential equations (PDEs) for these functions, in which system the (generally) time-dependent current that charges the capacitor appears as a sort of parametric function.

In the present article we suggest a mathematical process for obtaining solutions of the aforementioned system of PDEs in the form of power series with respect to time. This allows one to find approximate expressions for the e/m field in certain situations. For example, a slowly varying (thus almost time-independent) current allows for the “classical” solutions given in the literature, while a current that is almost linearly dependent on time (as may be assumed, in general, for any smoothly varying current in a very short time period) allows for new solutions that correct the standard expressions for the electric field while retaining the corresponding expressions for the magnetic field.

It should be noted that, regarding the solutions in the exterior of the capacitor, no retardation effects related to the finite speed of propagation of e/m interactions will concern us here. Indeed, as discussed in Sec. 4, our solutions are valid at points of

space not far from the capacitor, so that any change in the physical system will be felt “simultaneously” at all points of interest.

2. Solutions of Maxwell’s equations inside the capacitor

We consider a parallel-plate capacitor with circular plates of radius a , thus of area $A=\pi a^2$. The space in between the plates is assumed to be empty of matter. The capacitor is being charged by a time-dependent current $I(t)$ flowing in the $+z$ direction (see Fig. 1). The z -axis is perpendicular to the plates (the latter are therefore parallel to the xy -plane) and passes through their centers, as seen in the figure (by \hat{u}_z we denote the unit vector in the $+z$ direction).

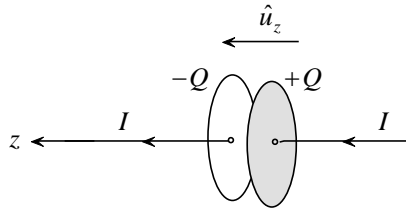


Figure 1

The capacitor is being charged at a rate $dQ/dt=I(t)$, where $+Q(t)$ is the charge on the right plate (as seen in the figure) at time t . If $\sigma(t)=Q(t)/\pi a^2=Q(t)/A$ is the surface charge density on the right plate, then the time derivative of σ is given by

$$\sigma'(t) = \frac{Q'(t)}{A} = \frac{I(t)}{A} \quad (1)$$

We assume that the plate separation is very small compared to the radius a , so that the e/m field inside the capacitor is practically independent of z , although it *does* depend on the normal distance ρ from the z -axis. In cylindrical coordinates (ρ, φ, z) the magnitude of the e/m field at any time t will thus only depend on ρ (due to the symmetry of the problem, this magnitude will not depend on the angle φ).

We assume that the positive and the negative plate of the capacitor of Fig. 1 are centered at $z=0$ and $z=d$, respectively, on the z -axis, where, as mentioned above, the plate separation d is much smaller than the radius a of the plates. The interior of the capacitor is then the region of space with $0 \leq \rho < a$ and $0 < z < d$.

The magnetic field inside the capacitor is azimuthal, of the form $\vec{B} = B(\rho, t)\hat{u}_\varphi$. A standard practice in the literature is to assume that, at all t , the electric field in this region is uniform, of the form

$$\vec{E} = \frac{\sigma(t)}{\epsilon_0} \hat{u}_z \quad (2)$$

while everywhere outside the capacitor the electric field vanishes. With this assumption the magnetic field inside the capacitor is found to be [4,5,8]

$$\vec{B} = \frac{\mu_0 I(t) \rho}{2\pi a^2} \hat{u}_\varphi = \frac{\mu_0 I(t) \rho}{2A} \hat{u}_\varphi \quad (3)$$

Expressions (2) and (3) must, of course, satisfy the Maxwell system of equations in empty space, which system we write in the form [3,10]

$$\begin{aligned} (a) \quad \vec{\nabla} \cdot \vec{E} &= 0 & (c) \quad \vec{\nabla} \times \vec{E} &= -\frac{\partial \vec{B}}{\partial t} \\ (b) \quad \vec{\nabla} \cdot \vec{B} &= 0 & (d) \quad \vec{\nabla} \times \vec{B} &= \varepsilon_0 \mu_0 \frac{\partial \vec{E}}{\partial t} \end{aligned} \quad (4)$$

By using cylindrical coordinates (see Appendix I) and by taking (1) into account, one may show that (2) and (3) satisfy three of Eqs. (4), namely, (a), (b) and (d). This is not the case with the Faraday-Henry law (4c), however, since by (2) and (3) we find that $\vec{\nabla} \times \vec{E} = 0$, while

$$\frac{\partial \vec{B}}{\partial t} = \frac{\mu_0 I'(t) \rho}{2A} \hat{u}_\varphi .$$

An exception occurs if the current I is constant in time, i.e., if the capacitor is being charged at a constant rate, so that $I'(t)=0$. This is actually the assumption silently or explicitly made in many textbooks (see, e.g., [4], Chap. 21). But, for a current $I(t)$ with arbitrary time dependence, the pair of fields (2) and (3) does not satisfy the third Maxwell equation.

To remedy the situation and restore the validity of the full set of Maxwell's equations in the interior of the capacitor, we must somehow correct the above expressions for the e/m field. To this end we employ the following *Ansatz*, taking into account Lemma 1 in Appendix II:

$$\begin{aligned} \vec{E} &= \left(\frac{\sigma(t)}{\varepsilon_0} + f(\rho, t) \right) \hat{u}_z , \\ \vec{B} &= \left(\frac{\mu_0 I(t) \rho}{2A} + g(\rho, t) \right) \hat{u}_\varphi ; \\ \sigma'(t) &= I(t)/A \end{aligned} \quad (5)$$

where $f(\rho, t)$ and $g(\rho, t)$ are functions to be determined consistently with the given current function $I(t)$ and the given initial conditions. It can be checked that the solutions (5) automatically satisfy the first two Maxwell equations (4a) and (4b). By the Faraday-Henry law (4c) and the Ampère-Maxwell law (4d) we get the following system of PDEs:

$$\begin{aligned}\frac{\partial f}{\partial \rho} &= \frac{\partial g}{\partial t} + \frac{\mu_0 I'(t) \rho}{2A} \\ \frac{1}{\rho} \frac{\partial(\rho g)}{\partial \rho} &= \varepsilon_0 \mu_0 \frac{\partial f}{\partial t}\end{aligned}\quad (6)$$

Note in particular that the “classical” solution with $f(\rho, t) \equiv 0$ and $g(\rho, t) \equiv 0$ is possible only if $I'(t) = 0$, i.e., if the current I is constant in time, which means that the capacitor is being charged at a constant rate.

The quantity $(1/\rho)\partial(\rho g)/\partial \rho$ in the second equation, having its origin at the expression for $\vec{\nabla} \times \vec{B}$ in cylindrical coordinates, must tend to a finite limit for $\rho \rightarrow 0$ in order that the *rot* of the magnetic field be finite at the center of the capacitor. For this to be the case, $\partial(\rho g)/\partial \rho$ must only contain terms of at least first order in ρ . This, in turn, requires that g itself must be of at least first order (i.e., linear with no constant term) in ρ for all t , or else g must be identically zero. We must, therefore, require that

$$g(\rho, t) \rightarrow 0 \text{ for } \rho \rightarrow 0 \quad (7)$$

for all t . Keeping this condition in mind, we can rewrite the system (6) in a more symmetric form:

$$\begin{aligned}\frac{\partial f}{\partial \rho} &= \frac{\partial g}{\partial t} + \frac{\mu_0 I'(t) \rho}{2A} \\ \frac{\partial(\rho g)}{\partial \rho} &= \varepsilon_0 \mu_0 \frac{\partial(\rho f)}{\partial t}\end{aligned}\quad (8)$$

In principle, one needs to solve the system (8) for a given current $I(t)$ and for given initial conditions. An alternative approach, leading to approximate solutions of various forms, is to expand all functions (i.e., f , g and I) in powers of time, t . We thus write:

$$I(t) = \sum_{n=0}^{\infty} I_n t^n \quad (9a)$$

$$f(\rho, t) = \sum_{n=0}^{\infty} f_n(\rho) t^n \quad (9b)$$

$$g(\rho, t) = \sum_{n=0}^{\infty} g_n(\rho) t^n \quad (9c)$$

Then, for example,

$$I'(t) = \sum_{n=1}^{\infty} n I_n t^{n-1} = \sum_{n=0}^{\infty} (n+1) I_{n+1} t^n, \text{ etc.}$$

Obviously, I_n has dimensions of current \times (time) $^{-n}$, while f_n and g_n have dimensions of field intensity (electric and magnetic, respectively) \times (time) $^{-n}$.

Substituting the series expansions (9) into the system (8), and equating coefficients of similar powers of t on both sides of the ensuing equations, we get a recursion relation in the form of a system of PDEs:

$$\begin{aligned} f_n'(\rho) &= (n+1) \left[g_{n+1}(\rho) + \frac{\mu_0 \rho}{2A} I_{n+1} \right] \\ [\rho g_n(\rho)]' &= (n+1) \varepsilon_0 \mu_0 \rho f_{n+1}(\rho) \end{aligned} \quad (10)$$

for $n=0,1,2,\dots$. All non-vanishing functions $g_n(\rho)$ are required to satisfy the boundary condition (7); i.e., $g_n(\rho) \rightarrow 0$ for $\rho \rightarrow 0$.

An obvious solution of the system (10) is the trivial solution $f_n(\rho) \equiv 0$ and $g_n(\rho) \equiv 0$ for all $n=0,1,2,\dots$, corresponding to $f(\rho,t) \equiv 0$ and $g(\rho,t) \equiv 0$. For this to be the case, we must have $I_{n+1} = 0$ for all $n=0,1,2,\dots$, which means that $I(t) = I_0 = \text{constant}$ (independent of t). This is the case typically treated in the literature, although the condition $I = \text{const.}$ is usually not stated explicitly.

The simplest nontrivial solution of the problem is found by assuming that f and g are time-independent, i.e., are functions of ρ only. Then, by (9b) and (9c), $f = f_0(\rho)$ and $g = g_0(\rho)$, while $f_n(\rho) = 0$ and $g_n(\rho) = 0$ for $n > 0$. The system (10) for $n=0$ gives

$$f_0'(\rho) = \frac{\mu_0 I_1 \rho}{2A} \quad \text{and} \quad [\rho g_0(\rho)]' = 0$$

with solutions

$$f_0(\rho) = \frac{\mu_0 I_1 \rho^2}{4A} + C \quad \text{and} \quad g_0(\rho) = \frac{\lambda}{\rho},$$

respectively. The boundary condition $g_0(\rho) \rightarrow 0$ for $\rho \rightarrow 0$ cannot be satisfied for $\lambda \neq 0$; we are thus compelled to set $\lambda = 0$. Given that $f(\rho,t) = f_0(\rho)$ and $g(\rho,t) = g_0(\rho)$, the solution of the system (8) is

$$f(\rho,t) = \frac{\mu_0 I_1 \rho^2}{4A} + C, \quad g(\rho,t) \equiv 0 \quad (11)$$

As is easy to check, by the first of Eqs. (10) it follows that $I_n = 0$ for $n > 1$. Therefore $I(t)$ is linear in t , i.e., is of the form $I(t) = I_0 + I_1 t$. By assuming the initial condition $I(0) = 0$, we have that $I_0 = 0$ and

$$I(t) = I_1 t \quad (12)$$

On the other hand, by integrating Eq. (1): $\sigma'(t) = I(t)/A$, and by assuming that the capacitor is initially uncharged [$\sigma(0) = 0$], we get:

$$\sigma(t) = \frac{I_1 t^2}{2A} \quad (13)$$

Finally, by Eqs. (5), (11), (12) and (13) the e/m field in the interior of the capacitor is

$$\begin{aligned}\vec{E} &= \left(\frac{I_1 t^2}{2\varepsilon_0 A} + \frac{\mu_0 I_1 \rho^2}{4A} \right) \hat{u}_z, \\ \vec{B} &= \frac{\mu_0 I_1 t \rho}{2A} \hat{u}_\varphi\end{aligned}\tag{14}$$

where we have set $C=0$ since, in view of the assumed initial conditions, there is no electric field inside the capacitor if $I_1=0$. In order for the solution (14) to be valid, the current $I(t)$ charging the capacitor must vary linearly with time, according to (12).

3. Solutions of Maxwell's equations outside the capacitor

We recall that the positive and the negative plate of the capacitor of Fig. 1 are centered at $z=0$ and $z=d$, respectively, on the z -axis, where the plate separation d is much smaller than the radius a of the plates. The space exterior to the capacitor consists of points with $\rho > 0$ and $z \notin (0, d)$, as well as points with $\rho > a$ and $0 < z < d$. (In the former case we exclude points on the z -axis, with $\rho=0$, to ensure the finiteness of our solutions in that region.) We assume that the current $I(t)$ is of "infinite" extent and hence the magnitude of the e/m field is practically z -independent.

The e/m field outside the capacitor is usually described mathematically by the equations [4,5,8]

$$\vec{E} = 0, \quad \vec{B} = \frac{\mu_0 I(t)}{2\pi\rho} \hat{u}_\varphi\tag{15}$$

As the case is with the standard solutions in the interior of the capacitor, the solutions (15) fail to satisfy the Faraday-Henry law (4c) (although they do satisfy the remaining three Maxwell equations), since $\vec{\nabla} \times \vec{E} = 0$ while

$$\frac{\partial \vec{B}}{\partial t} = \frac{\mu_0 I'(t)}{2\pi\rho} \hat{u}_\varphi.$$

As before, an exception occurs if the current I is constant in time, i.e., if the capacitor is being charged at a constant rate, so that $I'(t)=0$.

To find more general solutions that satisfy the entire set of the Maxwell equations, we work as in the previous section. Taking into account Lemma 2 in Appendix II, we assume the following general form of the e/m field everywhere outside the capacitor:

$$\begin{aligned}\vec{E} &= f(\rho, t) \hat{u}_z, \\ \vec{B} &= \left(\frac{\mu_0 I(t)}{2\pi\rho} + g(\rho, t) \right) \hat{u}_\varphi\end{aligned}\tag{16}$$

where f and g are functions to be determined consistently with the given current function $I(t)$. The solutions (16) automatically satisfy the first two Maxwell equations (4a) and (4b). By Eqs. (4c) and (4d) we get the following system of PDEs:

$$\begin{aligned}\frac{\partial f}{\partial \rho} &= \frac{\partial g}{\partial t} + \frac{\mu_0 I'(t)}{2\pi\rho} \\ \frac{\partial(\rho g)}{\partial \rho} &= \varepsilon_0 \mu_0 \frac{\partial(\rho f)}{\partial t}\end{aligned}\quad (17)$$

Again, the usual solution with $f(\rho, t) \equiv 0$ and $g(\rho, t) \equiv 0$ is possible only if $I'(t) = 0$, i.e., if the capacitor is being charged at a constant rate. Note also that, since now $\rho \neq 0$, the boundary condition (7) for g no longer applies.

As we did in the previous section, we seek a series solution of the system (17) in powers of t . We thus expand f , g and I as in Eqs. (9), substitute the expansions into the system (17), and compare terms with equal powers of t . The result is a new recursive system of PDEs:

$$\begin{aligned}f'_n(\rho) &= (n+1) \left[g_{n+1}(\rho) + \frac{\mu_0}{2\pi\rho} I_{n+1} \right] \\ [\rho g_n(\rho)]' &= (n+1) \varepsilon_0 \mu_0 \rho f_{n+1}(\rho)\end{aligned}\quad (18)$$

for $n=0, 1, 2, \dots$. Again, an obvious solution is the trivial solution $f_n(\rho) \equiv 0$ and $g_n(\rho) \equiv 0$ for all $n=0, 1, 2, \dots$, corresponding to $f(\rho, t) \equiv 0$ and $g(\rho, t) \equiv 0$. This requires that $I_{n+1} = 0$ for all $n=0, 1, 2, \dots$, so that $I(t) = I_0 = \text{constant}$ (independent of t).

As in Sec. 2, we seek time-independent solutions for f and g , so that $f = f_0(\rho)$ and $g = g_0(\rho)$ while $f_n(\rho) = 0$ and $g_n(\rho) = 0$ for $n > 0$. The system (18) for $n=0$ gives

$$f'_0(\rho) = \frac{\mu_0 I_1}{2\pi\rho} \quad \text{and} \quad [\rho g_0(\rho)]' = 0$$

with solutions

$$f_0(\rho) = \frac{\mu_0 I_1}{2\pi} \ln(\kappa\rho) \quad \text{and} \quad g_0(\rho) = \frac{\lambda}{2\pi\rho},$$

respectively (remember that $\rho > 0$), where κ is a positive constant quantity having dimensions of inverse length, and where a factor of 2π has been put in $g_0(\rho)$ for future convenience. Given that $f(\rho, t) = f_0(\rho)$ and $g(\rho, t) = g_0(\rho)$, the solution of the system (17) is

$$f(\rho, t) = \frac{\mu_0 I_1}{2\pi} \ln(\kappa\rho), \quad g(\rho, t) = \frac{\lambda}{2\pi\rho}\quad (19)$$

By the first of Eqs. (18) it follows that $I_n = 0$ for $n > 1$. Therefore $I(t)$ is linear in t , of the form $I(t) = I_0 + I_1 t$. By assuming the initial condition $I(0) = 0$, we have that $I_0 = 0$ and

$$I(t) = I_1 t \quad (20)$$

In view of the above results, the e/m field (16) in the exterior of the capacitor is

$$\begin{aligned} \vec{E} &= \frac{\mu_0 I_1}{2\pi} \ln(\kappa\rho) \hat{u}_z, \\ \vec{B} &= \frac{\mu_0 I_1 t + \lambda}{2\pi\rho} \hat{u}_\varphi \end{aligned} \quad (21)$$

For this solution to be valid, the current $I(t)$ must vary linearly with time.

By comparing Eqs. (14) and (21) we observe that the value of the electric field inside the capacitor does not match the value of this field outside for $\rho=a$, where a is the radius of the capacitor. This discontinuity of the electric field at the boundary of the space occupied by the capacitor is a typical characteristic of capacitor problems, in general. On the other hand, in order that the magnetic field in the strip $0 < z < d$ be continuous for $\rho=a$, the expression for \vec{B} in (21) must match the corresponding expression in (14) upon substituting $\rho=a$ and by taking into account that $A=\pi a^2$. This requires that we set $\lambda=0$ in (21), so that this equation finally becomes

$$\begin{aligned} \vec{E} &= \frac{\mu_0 I_1}{2\pi} \ln(\kappa\rho) \hat{u}_z, \\ \vec{B} &= \frac{\mu_0 I_1 t}{2\pi\rho} \hat{u}_\varphi \end{aligned} \quad (22)$$

4. Discussion

As we have seen, expressions for the e/m field inside and outside a charging capacitor may be sought in the general form given by Eqs. (5) and (16), respectively. These expressions contain two unknown functions $f(\rho,t)$ and $g(\rho,t)$ which, in view of Maxwell's equations, satisfy the systems of PDEs (8) and (17). These PDEs, in turn, admit series solutions in powers of t , of the form (9), where it is assumed that the current $I(t)$ itself may be expanded in this fashion.

The coefficients of expansion of f and g may be determined, in principle, by means of the recursion relations (10) and (18), both of which are of the general form

$$\begin{aligned} f_n'(\rho) &= (n+1)[g_{n+1}(\rho) + h(\rho)I_{n+1}] \\ [\rho g_n(\rho)]' &= (n+1)\varepsilon_0\mu_0\rho f_{n+1}(\rho) \end{aligned} \quad (23)$$

This is not an easy system to integrate, so we are compelled to make certain *ad hoc* assumptions. Suppose, e.g., that we seek a solution such that $f_n(\rho)=0$ and $g_n(\rho)=0$ for $n>k$ ($k\geq 0$). It then follows from the first of Eqs. (23) that $I_{n+1}=0$ for $n>k$ or, equivalently, $I_n=0$ for $n>k+1$. Thus, if $k=0$, $I(t)$ must be linear in t ; if $k=1$, $I(t)$ must be quadratic in t ; etc.

For a current varying sufficiently slowly with time, we may approximately assume that $I_n=0$ for $n>0$, so that $I(t)=I_0=const$. This allows for the possibility that f and g vanish identically, as is effectively assumed (though not always stated explicitly) in the literature. On the other hand, any smoothly varying $I(t)$ may be assumed to vary linearly with time for a very short time period. Then, a solution of the form (14) and (22) is admissible.

There are several aspects of the solutions described by Eqs. (14) and (22) that may look unphysical: (a) the electric field in (22) apparently diverges for $\rho \rightarrow \infty$; (b) the magnetic field in both (14) and (22) diverges for $t \rightarrow \infty$; (c) although, by assumption, there are no charges at the interface between the interior and the exterior of the capacitor (i.e., on the cylindrical surface defined by $0 < z < d$ and $\rho = a$) the electric field is non-continuous on that surface, contrary to the general boundary conditions required by Maxwell's equations; (d) the constant κ in (22) appears to be arbitrary. We may thus use the above solutions only as approximate ones for values of ρ not much larger than the radius a of the plates, as well as for short time intervals. (Note that ρ has to be much smaller than the length of the wire that charges the capacitor if this wire is to be considered of "infinite" length, hence if the external e/m field is to be regarded as z -independent.) We may smoothen the discontinuity problem of the electric field for $\rho = a$ by assuming that this field is continuous at $t=0$, i.e., at the moment when the charging of the capacitor begins. By setting $\rho = a$ in (14) and (22) and by equating the corresponding expressions for \vec{E} we may then determine the value of the constant κ in (22). The result is: $\kappa = e^{1/2}/a$.

For an enlightening discussion of the subtleties concerning the e/m field produced by an infinitely long straight current, the reader is referred to Example 7.9 of [3].

Appendix I. Vector operators in cylindrical coordinates

Let \vec{A} be a vector field, expressed in cylindrical coordinates (ρ, φ, z) as

$$\vec{A} = A_\rho(\rho, \varphi, z) \hat{u}_\rho + A_\varphi(\rho, \varphi, z) \hat{u}_\varphi + A_z(\rho, \varphi, z) \hat{u}_z .$$

The *div* and the *rot* of this field in this system of coordinates are written, respectively, as follows:

$$\vec{\nabla} \cdot \vec{A} = \frac{1}{\rho} \frac{\partial}{\partial \rho} (\rho A_\rho) + \frac{1}{\rho} \frac{\partial A_\varphi}{\partial \varphi} + \frac{\partial A_z}{\partial z} ,$$

$$\vec{\nabla} \times \vec{A} = \left(\frac{1}{\rho} \frac{\partial A_z}{\partial \varphi} - \frac{\partial A_\varphi}{\partial z} \right) \hat{u}_\rho + \left(\frac{\partial A_\rho}{\partial z} - \frac{\partial A_z}{\partial \rho} \right) \hat{u}_\varphi + \frac{1}{\rho} \left(\frac{\partial}{\partial \rho} (\rho A_\varphi) - \frac{\partial A_\rho}{\partial \varphi} \right) \hat{u}_z .$$

In particular, if the vector field is of the form

$$\vec{A} = A_\varphi(\rho)\hat{u}_\varphi + A_z(\rho)\hat{u}_z ,$$

then $\vec{\nabla} \cdot \vec{A} = 0$.

Appendix II. General form of the electric field

To justify the general expression for the electric field implied in the *Ansatz* (5) used to find solutions of Maxwell's equations inside the capacitor, we need to prove the following:

Lemma 1. If the magnetic field inside the capacitor is azimuthal, of the form

$$\vec{B} = B(\rho, t)\hat{u}_\varphi \tag{A.1}$$

then the electric field (also assumed dependent on ρ and t) is of the form

$$\vec{E} = E(\rho, t)\hat{u}_z \tag{A.2}$$

Proof. Let

$$\vec{E} = E_\rho(\rho, t)\hat{u}_\rho + E_\varphi(\rho, t)\hat{u}_\varphi + E_z(\rho, t)\hat{u}_z \tag{A.3}$$

Then (cf. Appendix I) from Gauss' law (4a) it follows that

$$\frac{\partial}{\partial \rho}(\rho E_\rho) = 0 \Rightarrow E_\rho \equiv \frac{\alpha(t)}{\rho} \tag{A.4}$$

In order for the electric field to be finite at the center of the capacitor (i.e., for $\rho=0$) we must set $\alpha(t)\equiv 0$, so that $E_\rho(\rho, t)=0$. On the other hand, the z -component of Faraday's law (4c) yields

$$\frac{\partial}{\partial \rho}(\rho E_\varphi) = 0 \Rightarrow E_\varphi \equiv \frac{\beta(t)}{\rho} \tag{A.5}$$

Again, finiteness of the electric field for $\rho=0$ dictates that $\beta(t)\equiv 0$, so that $E_\varphi(\rho, t)=0$. Eventually, only the z -component of the electric field is non-vanishing, in accordance with (A.2).

The solutions outside the capacitor are subject to the restriction $\rho>0$. The expression for the electric field implied in the *Ansatz* (16) is based on the following observation:

Lemma 2. If the magnetic field outside the capacitor is azimuthal, of the form (A.1), then the electric field (also assumed dependent on ρ and t) is again of the form (A.2).

Proof. Let the electric field be of the form (A.3). Then from Gauss' law (4a) and from the z -component of Faraday's law (4c) we get (A.4) and (A.5), respectively. On the other hand, from the ρ - and φ -components of the fourth Maxwell equation (4d) we find that $\partial E_\rho/\partial t=0$ and $\partial E_\varphi/\partial t=0$, which means that α and β are actually constants. Thus the general form of the electric field outside the capacitor should be

$$\vec{E} = \frac{\alpha}{\rho} \hat{u}_\rho + \frac{\beta}{\rho} \hat{u}_\varphi + f(\rho, t) \hat{u}_z .$$

Obviously, the function $f(\rho, t)$ is related to the time-change of the magnetic field and is expected to vanish if the current I that charges the capacitor is constant. If the electric field itself is to vanish when $I=constant$, both constants α and β must be zero. Eventually, the electric field outside the capacitor must be of the general form (A.2).

References

1. C. J. Papachristou, *Some remarks on the charging capacitor problem*, Advanced Electromagnetics, Vol. 7, No. 2 (2018) 10.¹
2. C. J. Papachristou, A. N. Magoulas, *On solving Maxwell's equations for a charging capacitor*, Nausivios Chora, Vol. 7 (2018) C-3.²
3. D. J. Griffiths, *Introduction to Electrodynamics*, 4th Edition (Pearson, 2013).
4. R. K. Wangsness, *Electromagnetic Fields*, 2nd Edition (Wiley, 1986).
5. A. Shadowitz, *The Electromagnetic Field* (McGraw-Hill, 1975).
6. V. Rojansky, *Electromagnetic Fields and Waves* (Dover, 1979).
7. J. D. Jackson, *Maxwell's displacement current revisited*, Eur. J. Phys. 20 (1999) 495.
8. K. T. McDonald, *Magnetic field in a time-dependent capacitor* (Princeton, 2017).
9. K. T. Selvan, *A revisiting of scientific and philosophical perspectives on Maxwell's displacement current*, IEEE Antennas and Propagation Magazine, Vol. 51, No. 3 (2009) 36.
10. C. J. Papachristou, *Introduction to Electromagnetic Theory and the Physics of Conducting Solids* (Springer, 2020).³

¹ <https://www.aemjournal.org/index.php/AEM/article/view/694>

² <https://nausivios.snd.edu.gr/docs/2018C1.pdf>

³ <https://arxiv.org/abs/1711.09969>

MULTICRITERIA OPTIMIZATION

Best Simultaneous Approximation of Functions

Alex Bacopoulos^a and Dimitra Kouloumpou^b

^a*Department of Applied Mathematics and Physical Sciences, National Technical University of Athens, Zografou Campus, 157 80, Athens, Greece, (abacop@central.ntua.gr)*

^b*Section of Mathematics, Mathematical Modeling and Applications Laboratory, Hellenic Naval Academy, Piraeus 18539, Greece, (dimkouloumpou@hna.gr)*

Abstract. The problem we consider is to find (the) **best approximation(s)** to a given function **simultaneously** with respect to more than one criterion of proximity. Questions of existence, characterization, unicity and computation are examined. Examples are given.

Keywords: Best vectorial approximation(s), minimal projection norms, computational schemata

1. INTRODUCTION

Among other formulations of simultaneous approximation, the notion of a "Vectorially Minimal Approximation" is introduced, which is shown to be the **natural setting** for problems of simultaneity, both theoretically as well as computationally. For the above formulations of Multicriteria Optimization we propose 3 types of "models" and show their interrelationships in each "primal" and "dual" spaces. In particular, attention has been given to effective models suitable for **numerical computation**. A related problem situated in the "dual space" of approximation operators is to approximate the (non-linear) **best approximation operator** by projection operators. This approach, as a tool of "good" approximation of functions (in situations to be specified), is motivated by the following inequality, where the role of minimal projections, i.e. $\min\|P\|$ is self-explanatory.

$$\|f - Pf\| \leq \|I - P\| \text{dist}(f, Y) \leq (1 + \|P\|) \text{dist}(f, Y).$$

Here again the approximation in the operator space is done **simultaneously** with respect to several norms. As just indicated, this reduces to finding "simultaneously" **minimal projection norms**. Examples are given and a "Zero in the Convex Hull" as well as a "Kolmogorov-type" characterization theorems are presented.

The tools used in this presentation are Elementary Optimization Theory, Computational Numerical Analysis and Elementary Functional Analysis.

2. VECTORIAL APPROXIMATION

Let $\|\cdot\|_a, \|\cdot\|_b$ be two norms defined on a linear space \mathcal{S} and let $f \in \mathcal{S} \sim \mathcal{K}$ be a given function to be approximated by approximation $p \in \mathcal{K} \subset \mathcal{S}$. \mathcal{K} is assumed to be a closed, convex, proper subset of \mathcal{S} . Let $G(p) = (\|f - p\|_a, \|f - p\|_b)$ and define the partial ordering \succeq on $G(\mathcal{K})$ by

$$G(p) \preceq G(q) \Leftrightarrow \begin{cases} \|f - p\|_a \leq \|f - q\|_a \\ \text{and} \\ \|f - p\|_b \leq \|f - q\|_b \end{cases}$$

We shall write $G(p) \prec G(q)$ if and only if $G(p) \preceq G(q)$ and $G(p) \neq G(q)$.

Definition 2.1

We say that p is a best vec approximation if there does not exist a $q \in \mathcal{K}$ such that $G(q) \prec G(p)$.

Definition 2.2

The minimal set M is given by

$$M = \{G(p): p \in \mathcal{K} \text{ is a best vec approximation}\}.$$

There are some general geometric facts that are easy to verify. We cite some of them here:

- $\pi_1(G(\mathcal{K}))$ has zero homotopy group.
- M is a convex, decreasing arc.

Let Λ is the 45° bisector of the $\|\cdot\|_a, \|\cdot\|_b$ orthogonal axes. L is the supporting line to $G(\mathcal{K})$ which makes 135° angle with $\|\cdot\|_a$ axes.

The proof of the following theorem is a consequence of the definitions, convexity and, in the case of $(P_m) = M \cup L$, the continuity of the best approximation operator. *Sum* here denotes the sum of two norms. *Max* means the maximum of two norms.

Theorem 2.1

Let p_s be a best *sum* approximation. Then $G(p_s) \subseteq M \cup L$. Similarly, if p_m denotes the best *max* approximation then $G(p_m) = M \cup L$ (assuming $M \cup L \neq \emptyset$).

Furthermore, we define the set D by

$$D = \left\{d: \inf_{q \in \mathcal{K}} \|f - q\|_a \leq d \leq \inf_{q \in B} \|f - q\|_a \right\}$$

where,

$$B = \left\{r \in \mathcal{K}: \|f - r\|_b = \inf_{q \in \mathcal{K}} \|f - q\|_b \right\}.$$

Theorem 2.2

An element $p \in K$ is a best vectorial approximation if and only if there exists $d \in D$ and $\Phi \in S^*$ satisfying

$$\|\Phi\|_b = 1$$

$$\Phi(f - b) = \|f - q\|_a \leq d$$

and

$$\operatorname{Re}\Phi(p - q) \leq 0 \text{ for all } q \in K \text{ satisfying } \|f - q\|_a \leq d.$$

3. VECTORIALY MINIMAL PROJECTIONS

Let $\Lambda = \Lambda(X, V)$ be the space of all linear operators from a real or complex space X into a finite-dimensional subspace V , and let Π be the family of all operators in Λ with a given fixed action on V (e.g., the identity action corresponds to the family of projections onto V). Let X be equipped with norms $\|\cdot\|_i, i = 1, 2, \dots, k$. Let X_i denote the normed space given by X with the norm $\|\cdot\|_i$, and define

$$\|x\| := (\|x\|_1, \|x\|_2, \dots, \|x\|_k).$$

Define the partial ordering " \preceq " on X by

$$\|x\| \preceq \|z\| \Leftrightarrow \|x\|_i \leq \|z\|_i \text{ for every } i = 1, 2, \dots, k.$$

We write $\|x\| \triangleleft \|z\|$ if and only if $\|x\| \preceq \|z\|$ and $\|x\| \neq \|z\|$.

Definition 3.1

For $Q \in \Lambda$, let $\|Q\|_i$ denote the operator norm on X_i , let

$\|Q\| := (\|Q\|_1, \|Q\|_2, \dots, \|Q\|_k)$ and define the partial ordering " \preceq " on Λ by

$$\|P\| \preceq \|Q\| \Leftrightarrow \|P\|_i \leq \|Q\|_i \text{ for every } i = 1, 2, \dots, k.$$

We write $\|P\| \triangleleft \|Q\|$ if and only if $\|P\| \preceq \|Q\|$ and $\|P\| \neq \|Q\|$.

P is a vectorially minimal operator in Π if there no exist $Q \in \Pi$ such that $\|Q\| \triangleleft \|P\|$.

Notation

The minimal set M is given by

$$M := \{\|P\| : P \in \Pi \text{ is a vectorially minimal operator in } \Pi\}.$$

Definition 3.2

For $i = 1, 2, \dots, k$ $(x, y) \in S(X_i^{**}) \times S(X_i^*)$ will be called an extremal pair for $Q \in \Lambda$, if $\langle Q_i^{**}x, y \rangle = \|Q\|_i$, where $Q_i^{**}: X_i^{**} \rightarrow V$ is the second adjoint extension of Q to X_i^{**} .

(S denotes the unit sphere).

Notation

Let $E(Q)$ be the set of all extremal pairs for Q . To each $(x, y) \in E(Q)$ associate the rank-one operator $y \otimes x$ from X_i to X_i^{**} given by $(y \otimes x)(z) = \langle z, y \rangle x$ for $z \in X_i$, where i is the subscript associated with (x, y) .

Theorem 3.1 (Characterization)

P has vectorially minimal norm in Π **if and only if** the closed convex hull of $\{y \otimes x\}_{(x,y) \in E(P)}$ contains an operator E_P for which V is an invariant subspace, i.e.

$$E_P = \int_{E(P)} y \otimes x d\mu(x, y) : V \rightarrow V.$$

Theorem 3.2

P has vectorially minimal norm in Π if and only if there does not exist $D \in \Delta = \{D \in \Lambda : D = 0 \text{ in } V\}$ such that

$$\sup_{(x,y) \in E(P)} \operatorname{Re} \langle P_i^{**} x, y \rangle \overline{\langle D^{**} x, y \rangle} < 0.$$

4. SOME SPECIAL CASES

We give some examples of **Theorem 2.2**. In the notation of this theorem, let $S = C[a, b]$,

$K = \Pi_n[a, b]$ (the set of polynomials on $[a, b]$ of degree less than or equal to n), $\|\cdot\|$ is the supremum norm on $[a, b]$ and $w_1, w_2 \in C[a, b]$ two (weight) functions, positive and continuous on $[a, b]$.

We introduce extreme points, for a given $f \in C[a, b]$ to be approximated, in connection with the next theorem, as follows:

$$\begin{aligned} \bar{X}_{+1} &= \{x \in [a, b] : w_1(x)(f(x) - p(x)) = +\|w_1(f - p)\|\} \\ \bar{X}_{+2} &= \{x \in [a, b] : w_2(x)(f(x) - p(x)) = +\|w_2(f - p)\|\} \\ \bar{X}_{-1} &= \{x \in [a, b] : w_1(x)(f(x) - p(x)) = -\|w_1(f - p)\|\} \\ \bar{X}_{-2} &= \{x \in [a, b] : w_2(x)(f(x) - p(x)) = -\|w_2(f - p)\|\}. \end{aligned}$$

$$\bar{X}_p = \bar{X}_{+1} \cup \bar{X}_{+2} \cup \bar{X}_{-1} \cup \bar{X}_{-2}$$

The sign function $\sigma(x)$ on \bar{X}_p is defined by

$$\sigma(x) = -1 \text{ when } x \in \bar{X}_{-1} \cup \bar{X}_{-2}$$

and

$$\sigma(x) = +1 \text{ when } x \in \bar{X}_{+1} \cup \bar{X}_{+2}.$$

Theorem 4.1 (Application)

Consider the Vectorial Chebyshev optimization, with w_1 and w_2 as defined above. Then p is a best vec approximation to f if and only if there exist $n + 2$ points $x_1 < x_2 < \dots < x_{n+2} \in \bar{X}_p \subset [a, b]$ satisfying

$$\sigma(x_i) = (-1)^{i+1} \sigma(x_1) \text{ for every } i = 1, 2, \dots, n + 2.$$

Theorem 4.2

Each best vec approximation is unique; i.e. given $\mu \in M$ there is only one $p \in \Pi_n[a, b]$ such that $G(p) = \mu$.

Note that this uniqueness does not contradict the fact that the minimal set M has, in general, an infinite number of points, each of which corresponds to a (unique) best vectorial approximation. Likewise, the easily shown existence of M proves the existence of best solutions.

Theorem 4.3 (Application)

Let $X = C[a, b]$, $K = \Pi_n[a, b]$, $\|\cdot\|_a, \|\cdot\|_b$ the *sup* and L_2 norms on $C[a, b]$ which we denote by $\|\cdot\|_\infty$ and $\|\cdot\|_2$ respectively.

Find the best vectorial approximation p_d whose error in Chebyshev norm equals a prescribed value $d \in P^+$, $\|f - p_1\|_\infty \leq d \leq \|f - p_2\|_\infty$. It is clear that the desired polynomial p_d is the unique solution to the problem

$$\min_{p \in \Pi_n} \|f - p\|_2$$

subject to

$$\|f - p\|_\infty \leq d.$$

Since the number of constraints here is infinite, we proceed by solving a sequence of quadratic programming problems, each with a finite number of constraints. The sequence of solutions $\{p_k\}$ is shown to converge to the theoretical solution p_d .

Algorithm Corresponding to Theorem 4.3

At the k – *th* step we have from the preceding steps a finite set of points $X^k \subset [a, b]$. We solve the quadratic program

$$\min_{p \in \Pi_n} \|f - p\|_2$$

subject to

$$\|f(x) - p(x)\|_\infty \leq d, x \in X_k.$$

Denoting by p_k the solution of this problem, we calculate a point $x_k \in [a, b]$ such that

$$|f(x_k) - p_k(x_k)| = \|f - p_k\|_\infty.$$

We form $X^{k+1} = X^k \cup \{x_k\}$ and proceed to the next cycle. At the beginning X^1 may be an arbitrary finite set, containing a maximum of $|f(x) - p_L(x)|$.

REFERENCES

1. S.M. Lozinski, On a class of linear operators, Dokl. Akad. Nauk SSSR 64, 1948, pp. 193-196.
1. E.W. Cheney, C.R. Hobby, P.D. Morris, F. Schurer and D.E. Wulbert, On the minimal property of the Fourier projection, Trans. Am. Math. Soc. 143, 1969, pp. 249-258.
2. E.W. Cheney and K.H. Price, Minimal projections, in Approximation Theory, Proceedings of Symposium, Lancaster 1969, New York 1971, pp. 261-289.
3. W. Odyniec and G. Lewicki, Minimal projections in Banach spaces, Springer-Verlag Lecture Notes in Mathematics, 1449.
5. D.H. Hyers, G. Isac and Th.M. Rassias, Topics in nonlinear analysis and applications, World Scientific, 1997.
6. B. Brosowski and A. Da Silva, Scalarization of vectorial relations applied to certain optimization problems, Note Mat. 11, 1991, pp. 69-91.
7. B.L. Chalmers and F.T. Metcalf, A characterization and equations for minimal projections and extensions, J. Operator Theory 32, 1994, pp. 31-46.
8. B.L. Chalmers and F.T. Metcalf, minimal projections and extensions for compact Abelian groups, in Approximation Theory VI, C.K. Chui et al., eds., Academic Press, 1989, pp. 129-132.
9. A. Bacopoulos and B.L. Chalmers, Vectorially minimal projections, in Approximation Theory III Vol. 1: Approximation and Interpolation, World Scientific, C.K. Chui and L.L. Schumaker, eds. 1995, pp. 15-22.
10. A. Bacopoulos and C.A. Botsaris, An efficient blend of the first Remes algorithm with quadratic programming, J. Math. Anal. Appl. 174, No. 2, 1993, pp. 342-358.
11. A. Bacopoulos, Computational n-D Optimization, BOOK in progress. Suggested to A. Bacopoulos by Richard Bellman (available R.B.'s letter)